INTERNATIONAL JOURNAL FOR NUMERICAL METHODS IN ENGINEERING
Int. J. Numer. Meth. Engng 2016; **00**:1–27
Published online in Wiley InterScience (www.interscience.wiley.com). DOI: 10.1002/nme

Stability-preserving model order reduction for time-domain simulation of vibro-acoustic FE models

A. van de Walle*,† , F. Naets, E. Deckers and W. Desmet

Department of Mechanical Engineering, KU Leuven, Celestijnenlaan 300B, B-3001 Heverlee, Leuven, Belgium

SUMMARY

This work proposes novel stability-preserving model order reduction approaches for vibro-acoustic finite element models. As most research in the past for these systems has focused on noise attenuation in the frequency-domain, stability-preserving properties were of low priority. However as the interest for time-domain auralization and (model based) active noise control increases, stability-preserving model order reduction techniques are becoming indispensable. The original finite element models for vibro-acoustic simulation are already well established, but require too much computational load for these applications. This work therefore proposes two new global approaches for the generation of stable reduced-order models. Based on proven conditions for stability preservation under one-sided projection, a reformulation of the displacement-fluid velocity potential ($u - \phi$) formulation is proposed. In contrast to the regular formulation, the proposed approach leads to a new asymmetric structure for the system matrices which is proven to preserve stability under one-sided projection. The second approach starts from a displacement-pressure ($u - p$) description where the system level projection space is decoupled for the two domains, for which we also prove the preservation of stability. Two numerical validation cases are presented which demonstrate the inadequacy of straightforward model order reduction on typical vibro-acoustic models for time-domain simulation and compare the performance of the proposed approaches. Both proposed approaches effectively preserve the stability of the original system. Copyright © 2016 John Wiley & Sons, Ltd.

Received ...

KEY WORDS: vibro-acoustics; finite element method; model reduction; stability

1. INTRODUCTION

Computer-aided engineering (CAE) tools have become indispensable in the modern design process. The ever-increasing customer demands regarding the acoustic performance of products therefore inspire the development of accurate and efficient methodologies for vibro-acoustic simulation. Conventional simulation methods analyze (vibro-)acoustic problems in the frequency-domain, but transient analysis in the time-domain is important to assess the product sound quality. This is why transient simulation techniques have received an increasing amount of attention in recent literature [1–7].

One of the most commonly used numerical methods in the field of vibro-acoustic simulation is the finite element (FE) method [8], which can be used in both frequency- and time-domain. Various finite element formulations exist for coupled vibro-acoustic problems. An overview of these formulations can be found in [9]. The most widespread formulation uses displacements as

*Correspondence to: A. van de Walle, Department of Mechanical Engineering, KU Leuven, Celestijnenlaan 300B, B-3001 Heverlee, Leuven, Belgium
†e-mail: axel.vandewalle@mech.kuleuven.be

nodal degrees of freedom in the structure and pressure in the fluid. We will refer to this formulation as the $u-p$ formulation. This is the most natural formulation for the coupled vibro-acoustic problem since the nodal degrees of freedom represent physical, measurable quantities. Another reason for the popularity of this formulation is that it results in a real dynamic stiffness matrix for undamped frequency-domain simulations and in a real eigenvalue problem for the computation of the undamped modes. It is the standard formulation used in most commercial FE tools for coupled vibro-acoustic analysis [10].

One of the major drawbacks of element-based methods is their computational cost, which scales unfavourably with increasing problem size and frequency, restricting the overall practical applicability. In order to accurately describe the wave-like spatial character of the variables, the use of locally defined and low-order shape functions imposes minimum requirements on the number of elements used per wavelength, and therefore limits the maximum element size for a given wavelength [11]. The highest frequency of interest determines the smallest wavelength present in the model, which in turn dictates the maximum element size. Because of the three-dimensional nature of acoustics, the number of elements in the model grows rapidly with increasing problem size or equivalently with decreasing element size (and thus also with increasing frequency). In order to alleviate the problems associated with computational costs one can turn to model order reduction (MOR) techniques to reduce the number of degrees of freedom for a desired accuracy [12]. For coupled vibro-acoustic problems the advantages of MOR have already been demonstrated in frequency-domain analysis [10, 13, 14]. In this paper we show that popular reduction techniques for frequency-domain analysis cannot be directly applied to time-domain analysis. This stems from the fact that these techniques generally do not preserve the stability of the original system in the reduced-order model (ROM). A loss of stability has no negative impact on the frequency-domain analysis of the system, but it leads to a rapidly diverging response in the time-domain.

Several general MOR techniques that preserve system stability have already been developed. Balanced truncation [15] ensures system stability, but the computational effort associated with solving the Lyapunov equations scales poorly with problem size ($\sim \mathcal{O}(n^3)$), making the application of balanced truncation infeasible for practical purposes. Recent works by Amsallem and Farhat [16] and Bond and Daniel [17] both present general purpose optimization approaches to obtain a stable reduced-order model. The right projection basis is left unchanged while the left projection basis is modified in order to achieve stability. In both works the constraints of the optimization problem enforce the stability of the reduced-order model while the objective function is chosen to minimize the difference between the resulting left projection basis and the original one to ensure that the loss of accuracy in the stabilization process is as small as possible. Yet the method described by Amsallem and Farhat in [16] does not guarantee the existence of a feasible (stable) solution. For the approach of Bond and Daniel in [17] the existence of a feasible solution can be proven, but the proposed algorithms are not guaranteed to find a feasible solution in a finite number of iterations. These are major drawbacks for the practical use of both methods. The method described by Kalashnikova et al. in [18] guarantees the stability of the resulting ROM through pole placement. This ensures that the resulting ROM is stable but leads to a trade-off on the accuracy where the loss is theoretically unbounded. In the field of circuit modeling and simulation there has also been a lot of attention for stability- and passivity-preserving MOR [19, 20]. However, because these methods rely on the specific structure of these circuit models, it is not possible to apply them to vibro-acoustic systems. An interesting alternative for passivity preserving MOR is interpolation of spectral zeros [21–23], but this technique is restricted to Krylov subspace methods and limits the choice of interpolation points.

This work proposes and compares two new approaches for reduced-order coupled vibro-acoustic FE simulation which inherently preserve the stability (and under the right circumstances even the passivity) of the original system. This makes the resulting reduced-order models suitable for time-domain simulation. These methods are computationally inexpensive and require only

DOI: 10.1002/nme

minor modifications to existing MOR schemes for frequency-domain vibro-acoustic analysis. We mathematically derive a set of sufficient conditions under which the stability of the coupled system is preserved in a one-sided projection. It is shown that the basic structure of the common $u-p$ and $u-\phi$ formulations for vibro-acoustics does not lead to preservation of stability in the reduced-order model.
The first of the proposed approaches is based on an altered $u-\phi$ formulation for vibro-acoustics. We prove that with a small but well-chosen modification to the $u-\phi$ formulation, the model loses symmetry but does however obtain a structure that is suitable for stability-preserving MOR. The results are general in the sense that any one-sided projection method can be applied.
The second approach is a direct application of block-structure preserving model order reduction. We prove that preserving the block-structure in the vibro-acoustic system matrices leads to stable reduced-order models. Again any one-sided projection method can be used, but the projection basis may need to be modified in order to ensure the preservation of the block-structure. This method enables stability-preserving model order reduction for vibro-acoustic systems in the $u-p$ formulation. The size of the reduced-order model is increased as compared to the first method.

This paper is structured as follows: Section 2 contains an introduction to the FE modeling of coupled vibro-acoustic systems. Next the projection-based MOR of these systems is discussed in section 3. Section 4 studies the conditions under which the one-sided projection of a linear descriptor system is guaranteed to retain stability. Particular emphasis is placed on the influence of definiteness of the system matrices. The insights obtained in this analysis are then used in section 5 to derive a strategy for performing one-sided projection-based MOR on a coupled vibro-acoustic system while preserving stability. We propose two alternative ways of formulating either the vibro-acoustic FE problem or its projection such that the requirements for preservation of stability are met. Next, the workflow for performing stability-preserving MOR is explained in section 6. Section 7 demonstrates the advantages of the proposed methods by reviewing several numerical experiments. Concluding remarks are made in section 8.

2. FINITE ELEMENT MODELING OF COUPLED VIBRO-ACOUSTIC SYSTEMS

The dynamics of a coupled vibro-acoustic system, spatially discretized using the finite element method, are described by the set of ordinary differential equations

$$\mathbf{M}\ddot{\mathbf{x}} + \mathbf{C}\dot{\mathbf{x}} + \mathbf{K}\mathbf{x} = \mathbf{F}, \tag{1}$$

where $\mathbf{M}$, $\mathbf{C}$ and $\mathbf{K} \in \mathbb{C}^{n\times n}$ are the mass, damping and stiffness matrices and $\mathbf{F} \in \mathbb{C}^n$ is the forcing vector. The total number of degrees of freedom is denoted as n and is the sum of the total number of structural degrees of freedom n_s and acoustic degrees of freedom n_a. Many methods exist to find a time-domain solution to this problem, provided that the forcing vector and the set of initial conditions are known [8]. We therefore concentrate on the continuous-time representation of the system.

As mentioned in the introduction, this system of equations can take on various forms depending on the formulation that is used to describe the coupled vibro-acoustic system. The most widespread formulation uses displacements in the structure u and pressure in the fluid p to characterize the state of the system. The full system of equations in this $u-p$ formulation is given by

$$\mathbf{M_{up}}\ddot{\mathbf{x}}_{\mathbf{up}} + \mathbf{C_{up}}\dot{\mathbf{x}}_{\mathbf{up}} + \mathbf{K_{up}}\mathbf{x_{up}} = \mathbf{F_{up}}, \tag{2}$$

with

DOI: 10.1002/nme

$$\mathbf{M_{up}} = \begin{bmatrix} \mathbf{M_s} & \mathbf{0} \\ -\rho\mathbf{K_c^T} & \mathbf{M_a} \end{bmatrix} \qquad \mathbf{C_{up}} = \begin{bmatrix} \mathbf{C_s} & \mathbf{0} \\ \mathbf{0} & \mathbf{C_a} \end{bmatrix} \qquad \mathbf{K_{up}} = \begin{bmatrix} \mathbf{K_s} & \mathbf{K_c} \\ \mathbf{0} & \mathbf{K_a} \end{bmatrix}$$
$$\mathbf{x_{up}} = \begin{bmatrix} \mathbf{u} \\ \mathbf{p} \end{bmatrix} \qquad \mathbf{F_{up}} = \begin{bmatrix} \mathbf{F_s} \\ \mathbf{F_a} \end{bmatrix}, \tag{3}$$

where $\mathbf{M_s}$, $\mathbf{C_s}$ and $\mathbf{K_s} \in \mathbb{C}^{n_s \times n_s}$ are the mass, damping and stiffness matrices of the structural part of the system, $\mathbf{M_a}$, $\mathbf{C_a}$ and $\mathbf{K_a} \in \mathbb{C}^{n_a \times n_a}$ are the mass, damping and stiffness matrices of the acoustic part of the system respectively, $\mathbf{K_c} \in \mathbb{C}^{n_s \times n_a}$ represents the vibro-acoustic coupling matrix and ρ is the specific density of the acoustic fluid [8]. The vector $\mathbf{u}$ contains the nodal displacements of the structure and $\mathbf{p}$ the nodal pressures in the acoustic fluid. The forcing vectors on the structural and acoustic part of the system are represented by $\mathbf{F_s} \in \mathbb{C}^{n_s}$ and $\mathbf{F_a} \in \mathbb{C}^{n_a}$ respectively. Since all of the submatrices in (3) originate from an FE discretization of structural dynamic and acoustic subsystems, $\mathbf{M_s}$ and $\mathbf{M_a}$ are symmetric positive definite, and $\mathbf{C_s}$, $\mathbf{C_a}$, $\mathbf{K_s}$ and $\mathbf{K_a}$ are symmetric positive (semi-)definite.

The $u-p$ formulation in (2)-(3) results in nonsymmetric global system matrices. Since symmetry can be a significant advantage when solving large sparse linear systems, Everstine [24] proposes an alternative, symmetric formulation which uses the scalar fluid velocity potential ϕ instead of the pressure p to describe the state of the fluid part of the system. This fluid velocity potential is defined by

$$p = -\rho\dot{\phi}, \tag{4}$$

such that the vector containing the nodal pressure values in the fluid can be expressed as $\mathbf{p} = -\rho\dot{\boldsymbol{\phi}}$. The use of this new state vector $\boldsymbol{\phi}$ for the fluid in conjunction with the state vector $\mathbf{u}$ for the structure results in what we will refer to as the $u-\phi$ formulation. The use of this $u-\phi$ formulation instead of the $u-p$ formulation results in the system of equations

$$\mathbf{M_{u\phi}}\ddot{\mathbf{x}}_{\mathbf{u\phi}} + \mathbf{C_{u\phi}}\dot{\mathbf{x}}_{\mathbf{u\phi}} + \mathbf{K_{u\phi}}\mathbf{x_{u\phi}} = \mathbf{F_{u\phi}}, \tag{5}$$

with

$$\mathbf{M_{u\phi}} = \begin{bmatrix} \mathbf{M_s} & \mathbf{0} \\ \mathbf{0} & -\rho\mathbf{M_a} \end{bmatrix} \qquad \mathbf{C_{u\phi}} = \begin{bmatrix} \mathbf{C_s} & -\rho\mathbf{K_c} \\ -\rho\mathbf{K_c^T} & -\rho\mathbf{C_a} \end{bmatrix} \qquad \mathbf{K_{u\phi}} = \begin{bmatrix} \mathbf{K_s} & \mathbf{0} \\ \mathbf{0} & -\rho\mathbf{K_a} \end{bmatrix}$$
$$\mathbf{x_{u\phi}} = \begin{bmatrix} \mathbf{u} \\ \boldsymbol{\phi} \end{bmatrix} \qquad \mathbf{F_{u\phi}} = \begin{bmatrix} \mathbf{F_s} \\ \mathbf{F_\phi} \end{bmatrix}, \tag{6}$$

where $\dot{\mathbf{F}}_{\boldsymbol{\phi}} = \mathbf{F_a}$. The global $\mathbf{K_{u\phi}}$, $\mathbf{C_{u\phi}}$ and $\mathbf{M_{u\phi}}$ matrices are now symmetric.

3. PROJECTION-BASED MOR FOR VIBRO-ACOUSTIC FE MODELS

The matrices in equation (1) are often very large in size, which severely limits its practical use due to computational constraints. To overcome this problem one can turn to MOR techniques to reduce the system size while still retaining a high level of accuracy. In projection-based MOR for systems described by (1), one attempts to find a left projection matrix $\mathbf{W} \in \mathbb{C}^{n \times r}$ and a right projection matrix $\mathbf{V} \in \mathbb{C}^{n \times r}$ such that the projected system

$$\mathbf{M_r}\ddot{\hat{\mathbf{x}}} + \mathbf{C_r}\dot{\hat{\mathbf{x}}} + \mathbf{K_r}\hat{\mathbf{x}} = \mathbf{F_r}, \tag{7}$$

with

DOI: 10.1002/nme

$$\begin{aligned} \mathbf{M_r} &= \mathbf{W^T M V} \qquad \mathbf{C_r} = \mathbf{W^T C V} \\ \mathbf{K_r} &= \mathbf{W^T K V} \qquad \mathbf{F_r} = \mathbf{W^T F} \\ \mathbf{x} &= \mathbf{V}\hat{\mathbf{x}}, \end{aligned} \tag{8}$$

is an accurate low-dimensional ($r \ll n$) approximation of the original system, in the sense that the input-output behaviour of the projected system resembles the one of the original system [12].

In order to perform a meaningful time-domain analysis of (1) by using the ROM in (7)-(8), it is essential that this ROM has the same stability properties as the original system in (1). Unfortunately preservation of stability is generally not ensured for this model order reduction process [25]. It is possible that the ROM is unstable even though the original system was stable.

In case $\mathbf{V} = \mathbf{W}$ the projection in (8) is called a *one-sided* projection. When $\mathbf{V} \neq \mathbf{W}$ it is called a *two-sided* projection [25]. In this work we present a *one-sided* projection framework that is guaranteed to preserve the stability properties of the original vibro-acoustic system.

It is difficult to directly study the stability of a second-order system as in (1) or its reduced-order counterpart in (7). We therefore introduce the concept of a linear descriptor system since criteria for stability are well-established for this kind of system. The dynamics of a linear descriptor system are governed by the set of equations

$$\begin{aligned} \mathbf{E}\dot{\mathbf{x}}_\mathbf{d} &= \mathbf{A}\mathbf{x}_\mathbf{d} + \mathbf{B}\mathbf{u} \\ \mathbf{y} &= \mathbf{L}\mathbf{x}_\mathbf{d}, \end{aligned} \tag{9}$$

with $\mathbf{E}, \mathbf{A} \in \mathbb{C}^{m\times m}$, $\mathbf{B} \in \mathbb{C}^{m\times k}$ and $\mathbf{L} \in \mathbb{C}^{\ell\times m}$, where $\mathbf{x_d} \in \mathbb{C}^m$ contains the states of the system, $\mathbf{u} \in \mathbb{C}^k$ the inputs to the system and $\mathbf{y} \in \mathbb{C}^\ell$ contains the outputs. It is important to note that the second-order system of equations in (1) can be written as such a first-order descriptor system:

$$\begin{aligned} \begin{bmatrix} \mathbf{I} & \mathbf{0} \\ \mathbf{0} & \mathbf{M} \end{bmatrix} \begin{bmatrix} \dot{\mathbf{x}} \\ \ddot{\mathbf{x}} \end{bmatrix} &= \begin{bmatrix} \mathbf{0} & \mathbf{I} \\ -\mathbf{K} & -\mathbf{C} \end{bmatrix} \begin{bmatrix} \mathbf{x} \\ \dot{\mathbf{x}} \end{bmatrix} + \begin{bmatrix} \mathbf{I} & \mathbf{0} \\ \mathbf{0} & \mathbf{I} \end{bmatrix} \begin{bmatrix} \mathbf{0} \\ \mathbf{F} \end{bmatrix} \\ \mathbf{y} &= \begin{bmatrix} \mathbf{I} & \mathbf{0} \\ \mathbf{0} & \mathbf{I} \end{bmatrix} \begin{bmatrix} \mathbf{x} \\ \dot{\mathbf{x}} \end{bmatrix}. \end{aligned} \tag{10}$$

The descriptor system in (9) can also be approximated using projection-based MOR in the same way as the second-order system in (1) is approximated by the projected system (7)-(8). We define the *one-sided* projection of the linear descriptor system in (9) as

$$\begin{aligned} \mathbf{E_r}\dot{\hat{\mathbf{x}}}_\mathbf{d} &= \mathbf{A_r}\hat{\mathbf{x}}_\mathbf{d} + \mathbf{B_r}\mathbf{u} \\ \mathbf{y} &= \mathbf{L_r}\hat{\mathbf{x}}_\mathbf{d}, \end{aligned} \tag{11}$$

with

$$\begin{aligned} \mathbf{E_r} &= \mathbf{V_d^T E V_d} \qquad \mathbf{A_r} = \mathbf{V_d^T A V_d} \\ \mathbf{B_r} &= \mathbf{V_d^T B} \qquad\quad \mathbf{L_r} = \mathbf{L V_d} \\ \mathbf{x_d} &= \mathbf{V_d}\hat{\mathbf{x}}_\mathbf{d}, \end{aligned} \tag{12}$$

and $\mathbf{V_d} \in \mathbb{C}^{m\times r}$, $\mathbf{E_r}, \mathbf{A_r} \in \mathbb{C}^{r\times r}$, $\mathbf{B_r} \in \mathbb{C}^{r\times k}$, $\mathbf{L_r} \in \mathbb{C}^{\ell\times r}$ and $\hat{\mathbf{x}}_\mathbf{d} \in \mathbb{C}^r$.

DOI: 10.1002/nme

The one-sided projection of the second-order system of equations (1) onto the basis $\mathbf{V}$ in (7)-(8), is equivalent to the projection of its descriptor system representation (10) onto the projection basis $\mathbf{V_d}$ in (11)-(12), with:

$$\mathbf{V_d} = \begin{bmatrix} \mathbf{V} & \mathbf{0} \\ \mathbf{0} & \mathbf{V} \end{bmatrix}. \tag{13}$$

Such a way of using a split basis is often referred to as *structure-preserving* model order reduction since the second-order structure of the system is preserved in the reduction process [26–29]. Note that it is also possible to use MOR techniques for first-order systems with the descriptor representation in (10), but this results in a projection matrix $\mathbf{V_d}$ which does not have the split structure from (13). Therefore the second-order structure of the system would be lost in such a first-order reduction process.

4. STABILITY OF THE ONE-SIDED PROJECTION OF A LINEAR DESCRIPTOR SYSTEM

The stability of a vibro-acoustic system is critical for its time-domain behaviour. In order to design stability-preserving MOR methods for vibro-acoustic FE models, we investigate the mathematical conditions under which a system is stable. For linear descriptor systems, stability criteria are well-established. This section therefore studies the conditions under which it is possible to preserve the stability of a linear descriptor system in a one-sided projection. The findings from this section will be exploited in section 5 to develop stability-preserving MOR methods for vibro-acoustic FE models.

The system in (9) is *critically stable* if and only if all of the generalized eigenvalues of the matrix pair $(\mathbf{A}, \mathbf{E})$ have a negative real part [30]. Since these eigenvalues correspond to the poles of the system, this is equivalent to stating that all the system poles must be in the closed left-half complex plane for the system to be critically stable. In the remainder of this article, the use of the term *stability* always refers to *critical stability*.

In this work, preservation of system stability in model reduction relies heavily on the definiteness properties of the system matrices. In this context, we define definiteness without the usual assumption of symmetry:

Definition 1
A matrix $\mathbf{Q} \in \mathbb{R}^{n \times n}$ is positive semi-definite if

$$\mathbf{x^T Q x} \geq 0$$

for any non-zero vector $\mathbf{x} \in \mathbb{R}^n$.

For positive definiteness the inequality in definition 1 becomes strict. Negative (semi-)definiteness is defined in the same manner. For matrices with non-real entries, the definition is extended by making use of the conjugate transpose (denoted by $\mathbf{x}^*$) and demanding that $\mathfrak{Re}\{\mathbf{x}^* \mathbf{Q x}\} \geq 0$ for any non-zero vector $\mathbf{x} \in \mathbb{C}^n$. For the sake of brevity, we will adopt $\mathbf{Q} > 0$ as a shorthand notation to indicate positive definiteness of the matrix $\mathbf{Q}$.

Theorem 1
A linear descriptor system as in (9) is stable if $\mathbf{E} = \mathbf{E^T} > 0$ and $\mathbf{A} \leq 0$.

Proof
This proof assumes that $\mathbf{E}, \mathbf{A} \in \mathbb{R}^{m \times m}$ in order not to overload the notation, but the proof can be extended to include matrices with non-real entries. Let $\lambda = a + bj$ be a generalized eigenvalue of the matrix pair $(\mathbf{A}, \mathbf{E})$ and $\boldsymbol{\phi} = \mathbf{u} + \mathbf{v}j$ the corresponding normalized eigenvector. By definition of

Prepared using nmeauth.cls
DOI: 10.1002/nme

the generalized eigenvalue problem, it holds that

$$\begin{aligned}
&\mathbf{A}\boldsymbol{\phi} = \lambda\mathbf{E}\boldsymbol{\phi} \\
\Leftrightarrow\ &(\mathbf{A} - \lambda\mathbf{E})\,\boldsymbol{\phi} = \mathbf{0} \\
\Leftrightarrow\ &(\mathbf{A} - a\mathbf{E} - b\mathbf{E}j)\,(\mathbf{u} + \mathbf{v}j) = \mathbf{0} \\
\Leftrightarrow\ &(\mathbf{A}\mathbf{u} - a\mathbf{E}\mathbf{u} + b\mathbf{E}\mathbf{v}) + (\mathbf{A}\mathbf{v} - a\mathbf{E}\mathbf{v} - b\mathbf{E}\mathbf{u})\,j = \mathbf{0} \\
\Leftrightarrow\ &\mathbf{A}\mathbf{u} - a\mathbf{E}\mathbf{u} + b\mathbf{E}\mathbf{v} = \mathbf{0} \qquad (\diamondsuit) \\
\textit{and}\ \ &\mathbf{A}\mathbf{v} - a\mathbf{E}\mathbf{v} - b\mathbf{E}\mathbf{u} = \mathbf{0} \qquad (\square).
\end{aligned}$$

Combining these two equations, we obtain

$$\begin{aligned}
&\mathbf{u}^{\mathbf{T}}(\diamondsuit) + \mathbf{v}^{\mathbf{T}}(\square) = 0 \\
\Leftrightarrow\ \ &a = \frac{\mathbf{u}^{\mathbf{T}}\mathbf{A}\mathbf{u} + \mathbf{v}^{\mathbf{T}}\mathbf{A}\mathbf{v}}{\mathbf{u}^{\mathbf{T}}\mathbf{E}\mathbf{u} + \mathbf{v}^{\mathbf{T}}\mathbf{E}\mathbf{v}}.
\end{aligned}$$

Since $\mathbf{A} \leq 0$ and $\mathbf{E} > 0$, definition 1 implies that $a \leq 0$. The real part of any generalized eigenvalue λ of this matrix pair $(\mathbf{A}, \mathbf{E})$ is always negative. The system is stable. □

A special class of linear descriptor systems called *definite systems* possesses some interesting properties regarding stability and also passivity. Passivity implies that the system does not generate energy.

Definition 2
The descriptor system in (9) is a definite system if and only if $\mathbf{E} = \mathbf{E}^{\mathbf{T}} > 0$, $\mathbf{A} \leq 0$ and $\mathbf{L} = \mathbf{B}^{\mathbf{T}}$.

Theorem 1 indicates that definite systems are always stable. Additionally, definite systems are also passive. The reader is referred to [31] for a proof.

Lemma 1
A congruence transformation of full rank retains definiteness.

Proof
Let $\mathbf{R} \in \mathbb{R}^{r\times r}$ be the result of a congruence transformation $\mathbf{S} \in \mathbb{R}^{n\times r}$ on a matrix $\mathbf{Q} \in \mathbb{R}^{n\times n}$ with $r < n$ and $rank(\mathbf{S}) = r$:

$$\mathbf{R} = \mathbf{S}^{\mathbf{T}}\mathbf{Q}\mathbf{S}.$$

For any vector $\mathbf{x} \in \mathbb{R}^n$ and corresponding $\mathbf{y} = \mathbf{S}\mathbf{x} \in \mathbb{R}^r$ it holds that

$$\mathbf{x}^{\mathbf{T}}\mathbf{R}\mathbf{x} = \mathbf{x}^{\mathbf{T}}\left(\mathbf{S}^{\mathbf{T}}\mathbf{Q}\mathbf{S}\right)\mathbf{x} = \left(\mathbf{x}^{\mathbf{T}}\mathbf{S}^{\mathbf{T}}\right)\mathbf{Q}\left(\mathbf{S}\mathbf{x}\right) = (\mathbf{S}\mathbf{x})^{\mathbf{T}}\mathbf{Q}(\mathbf{S}\mathbf{x}) = \mathbf{y}^{\mathbf{T}}\mathbf{Q}\mathbf{y}.$$

Through the use of definition 1, we can see that the definiteness of $\mathbf{Q}$ and $\mathbf{R}$ is equal. □

Note that this proof can be modified to include matrices with non-real entries, by replacing the regular transpose $^{\mathbf{T}}$ with the conjugate transpose *.

Now we have all the prerequisites to state and prove a theorem concerning the preservation of stability in MOR for linear descriptor systems.

Theorem 2
Stability is preserved in the one-sided projection of the descriptor system in (9) if $\mathbf{E} = \mathbf{E}^{\mathbf{T}} > 0$ and $\mathbf{A} \leq 0$.

Proof
To prove the theorem it suffices to show that the projected system (11)-(12) is stable under the conditions mentioned in the theorem.
Since $\mathbf{E} > 0$ and $\mathbf{A} \leq 0$, lemma 1 implies that also $\mathbf{E_r} > 0$ and $\mathbf{A_r} \leq 0$. Since $\mathbf{E} = \mathbf{E}^{\mathbf{T}}$ also $\mathbf{E_r} = \mathbf{V}^{\mathbf{T}}\mathbf{E}\mathbf{V} = \left(\mathbf{V}^{\mathbf{T}}\mathbf{E}\mathbf{V}\right)^{\mathbf{T}} = \mathbf{E}_{\mathbf{r}}^{\mathbf{T}}$. Then according to theorem 1, the projected system is stable. □

Note that since $\mathbf{L} = \mathbf{B}^{\mathbf{T}}$ implies $\mathbf{L_r} = \mathbf{B}_{\mathbf{r}}^{\mathbf{T}}$, a definite system as in definition 2 remains definite after a one-sided projection, retaining not only stability but also passivity.

DOI: 10.1002/nme

5. A STABILITY-PRESERVING ONE-SIDED PROJECTION FOR COUPLED VIBRO-ACOUSTIC FE MODELS

In this section the conditions for stability from the previous section are exploited in order to design stability-preserving model order reduction schemes for vibro-acoustic FE models.

As discussed in section 2, the matrices $\mathbf{K_s}$ and $\mathbf{K_a}$ originate from an FE discretization of structural and acoustic domains. Consequently they are symmetric and can be either positive definite or positive semi-definite. In case they are positive semi-definite, the zero eigenvalues of these matrices correspond to rigid body modes of the system. These rigid body modes manifest themselves as system poles at the origin of the complex plane. Since these poles are not in the open right-half plane they do not adversely affect the stability of the system. This is why we disregard the existence of rigid body modes in the subsequent analysis without loss of generality. This implies that we can consider $\mathbf{K_s}$ and $\mathbf{K_a}$ to be strictly positive definite.

To assess the possibility of retaining stability in a one-sided projection, we investigate the definiteness of the global system matrices. For the $u-p$ formulation in (2)-(3), $\mathbf{C_{up}}$ is positive (semi-)definite. However, $\mathbf{K_{up}}$ is not positive definite due to the presence of $\mathbf{K_c}$:

$$\begin{aligned}\mathbf{x^T K_{up} x} &= \begin{bmatrix}\mathbf{x_1^T} & \mathbf{x_2^T}\end{bmatrix}\begin{bmatrix}\mathbf{K_s} & \mathbf{K_c}\\ \mathbf{0} & \mathbf{K_a}\end{bmatrix}\begin{bmatrix}\mathbf{x_1}\\ \mathbf{x_2}\end{bmatrix}\\ &= \mathbf{x_1^T K_s x_1} + \mathbf{x_2^T K_a x_2} + \mathbf{x_1^T K_c x_2}.\end{aligned} \tag{14}$$

A similar observation can be made for $\mathbf{M_{up}}$.

Since $\mathbf{M_{up}}$ and $\mathbf{K_{up}}$ are indefinite, $\mathbf{E_{up}}$ and $\mathbf{A_{up}}$ of the equivalent descriptor system (10) are indefinite as well. It is possible that even though the vibro-acoustic system is stable, this stability is lost in a one-sided projection.

By contrast, the $u-\phi$ formulation in (5)-(6) has symmetric mass and stiffness matrices $\mathbf{M_{u\phi}}$ and $\mathbf{K_{u\phi}}$ in which $\mathbf{K_c}$ is no longer present. However, they are still indefinite:

$$\begin{aligned}\mathbf{x^T K_{u\phi} x} &= \begin{bmatrix}\mathbf{x_1^T} & \mathbf{x_2^T}\end{bmatrix}\begin{bmatrix}\mathbf{K_s} & \mathbf{0}\\ \mathbf{0} & -\rho\mathbf{K_a}\end{bmatrix}\begin{bmatrix}\mathbf{x_1}\\ \mathbf{x_2}\end{bmatrix}\\ &= \mathbf{x_1^T K_s x_1} - \rho\mathbf{x_2^T K_a x_2}.\end{aligned} \tag{15}$$

Again the $\mathbf{E_{u\phi}}$ and $\mathbf{A_{u\phi}}$ matrices of the equivalent descriptor system are indefinite such that stability is not preserved in a one-sided projection.

Even though the original vibro-acoustic system is stable, both the $u-p$ formulation in (2)-(3) and the $u-\phi$ formulation in (5)-(6) may result in reduced-order models that are unstable. In the following subsection we present a modification to the $u-\phi$ formulation that partially destroys the symmetry but nevertheless guarantees the stability of the reduced-order model.

5.1. Preservation of stability using a modified $u-\phi$ formulation

Although the $u-\phi$ formulation in (5)-(6) is symmetric, the global system matrices $\mathbf{M_{u\phi}}$ and $\mathbf{K_{u\phi}}$ are still indefinite. A change of sign of the set of equations governing the acoustic degrees of freedom remedies this. We will refer to this formulation as the *modified $u-\phi$ formulation*:

$$\mathbf{M_{mu\phi}\ddot{x}_{u\phi} + C_{mu\phi}\dot{x}_{u\phi} + K_{mu\phi}x_{u\phi} = F_{mu\phi}}, \tag{16}$$

with

DOI: 10.1002/nme

$$\mathbf{M_{mu\phi}} = \begin{bmatrix} \mathbf{M_s} & \mathbf{0} \\ \mathbf{0} & \rho\mathbf{M_a} \end{bmatrix} \qquad \mathbf{C_{mu\phi}} = \begin{bmatrix} \mathbf{C_s} & -\rho\mathbf{K_c} \\ \rho\mathbf{K_c^T} & \rho\mathbf{C_a} \end{bmatrix} \qquad \mathbf{K_{mu\phi}} = \begin{bmatrix} \mathbf{K_s} & \mathbf{0} \\ \mathbf{0} & \rho\mathbf{K_a} \end{bmatrix}$$
$$\mathbf{x_{u\phi}} = \begin{bmatrix} \mathbf{u} \\ \boldsymbol{\phi} \end{bmatrix} \qquad \mathbf{F_{mu\phi}} = \begin{bmatrix} \mathbf{F_s} \\ -\mathbf{F_\phi} \end{bmatrix}, \tag{17}$$

The global $\mathbf{M_{mu\phi}}$ and $\mathbf{K_{mu\phi}}$ matrices are now symmetric positive definite. The damping matrix $\mathbf{C_{mu\phi}}$ is no longer symmetric, but it is positive (semi-)definite:

$$\begin{aligned} \mathbf{x^T C_{mu\phi} x} &= \begin{bmatrix} \mathbf{x_1^T} & \mathbf{x_2^T} \end{bmatrix} \begin{bmatrix} \mathbf{C_s} & -\rho\mathbf{K_c} \\ \rho\mathbf{K_c^T} & \mathbf{C_a} \end{bmatrix} \begin{bmatrix} \mathbf{x_1} \\ \mathbf{x_2} \end{bmatrix} \\ &= \mathbf{x_1^T C_s x_1} + \mathbf{x_2^T C_a x_2} - \rho\mathbf{x_1^T K_c x_2} + \rho\mathbf{x_2^T K_c^T x_1} \\ &= \mathbf{x_1^T C_s x_1} + \mathbf{x_2^T C_a x_2} \geq 0. \end{aligned}$$

We now use the equivalent descriptor representation of the system in (16)-(17) to study its stability. The descriptor representation can be formulated as:

$$\begin{bmatrix} \mathbf{K_{mu\phi}^T} & \mathbf{0} \\ \mathbf{0} & \mathbf{M_{mu\phi}} \end{bmatrix} \begin{bmatrix} \dot{\mathbf{x}} \\ \ddot{\mathbf{x}} \end{bmatrix} = \begin{bmatrix} \mathbf{0} & \mathbf{K_{mu\phi}^T} \\ -\mathbf{K_{mu\phi}} & -\mathbf{C_{mu\phi}} \end{bmatrix} \begin{bmatrix} \mathbf{x} \\ \dot{\mathbf{x}} \end{bmatrix} + \begin{bmatrix} \mathbf{I} & \mathbf{0} \\ \mathbf{0} & \mathbf{I} \end{bmatrix} \begin{bmatrix} \mathbf{0} \\ \mathbf{F_{mu\phi}} \end{bmatrix}$$
$$\mathbf{y} = \begin{bmatrix} \mathbf{I} & \mathbf{0} \\ \mathbf{0} & \mathbf{I} \end{bmatrix} \begin{bmatrix} \mathbf{x} \\ \dot{\mathbf{x}} \end{bmatrix}, \tag{18}$$

with $\mathbf{E_{mu\phi}} = \mathbf{E_{mu\phi}^T} > 0$ and with $\mathbf{A_{mu\phi}} \leq 0$, as for any $\mathbf{x} = \begin{bmatrix} \mathbf{x_1} \\ \mathbf{x_2} \end{bmatrix} \neq \mathbf{0}$:

$$\begin{aligned} \mathbf{x^T A_{mu\phi} x} &= \begin{bmatrix} \mathbf{x_1^T} & \mathbf{x_2^T} \end{bmatrix} \begin{bmatrix} \mathbf{0} & \mathbf{K_{mu\phi}^T} \\ -\mathbf{K_{mu\phi}} & -\mathbf{C_{mu\phi}} \end{bmatrix} \begin{bmatrix} \mathbf{x_1} \\ \mathbf{x_2} \end{bmatrix} \\ &= -\mathbf{x_2^T C_{mu\phi} x_2} + \mathbf{x_1^T K_{mu\phi}^T x_2} - \mathbf{x_2^T K_{mu\phi} x_1} \\ &= -\mathbf{x_2^T C_{mu\phi} x_2} \\ &\leq 0, \end{aligned}$$

since $\mathbf{C_{mu\phi}} \geq 0$.

Using the equivalent descriptor formulation in (18) to study the stability of the the modified $u-\phi$ formulation in (16)-(17), we see that $\mathbf{E_{mu\phi}} = \mathbf{E_{mu\phi}^T} > 0$ and $\mathbf{A_{mu\phi}} \leq 0$. According to theorem 2, the stability of this system is preserved in a one-sided projection. Actually, since $\mathbf{L_{mu\phi}} = \mathbf{B_{mu\phi}^T}$, this is even a definite system, guaranteeing not only stability but also passivity.

The modified $u-\phi$ formulation (16)-(17) of a vibro-acoustic FE model, even though it lacks some symmetry compared to the standard $u-\phi$ formulation in (5)-(6), guarantees that a one-sided projection-based MOR procedure as in (7)-(8) preserves stability. The resulting reduced-order models are therefore well-suited for time-domain simulation.

Note that in vibro-acoustic simulations the pressure p is the quantity of physical interest in the acoustic domain. When performing simulations using the modified $u-\phi$ formulation p can be obtained directly without the need for extensive post-processing. In cases where the first-order state-space representation (10) is used the nodal values $\dot{\boldsymbol{\phi}}$ are part of the state vector, and the vector $\mathbf{p}$ is found through the relationship $\mathbf{p} = -\rho\dot{\boldsymbol{\phi}}$. When simulating the system in its second-order formulation (1) common time-integration schemes (e.g. those of the Newmark-family [32]) also explicitly calculate the time derivative of the primary variables. In these cases, obtaining $\mathbf{p}$ requires no additional computational cost.

DOI: 10.1002/nme

5.2. Preservation of stability using the $u-p$ formulation and extended projection basis

The previous section introduces a modification to the $u-\phi$ formulation and proves that this modification ensures stability preservation in a one-sided projection. This requires that the problem is (re)formulated with the fluid velocity potential ϕ as primary variable in the fluid domain. Although there is no theoretical barrier for doing so, we already argued that the $u-p$ formulation is the most widespread. With the insights gained in the properties of the (modified) $u-\phi$ formulation, we now develop a method to reduce the model in $u-p$ formulation with preservation of stability. The main drawback of this method is that the reduced-order model may double in size as compared to the first method using the modified $u-\phi$ formulation. We therefore stress that the method established in section 5.1 is theoretically superior, but the method developed in this section holds the practical advantage that the system can be kept in the more conventional $u-p$ formulation. The structural and fluid degrees of freedom are kept separate in the reduced-order model, which enables the use of staggered time integration schemes. When implemented in a parallel fashion this may (partially) compensate for the increase in ROM size.

The starting point for this stability-preserving MOR strategy for the system in $u-p$ formulation is an equivalence between the poles of the $u-p$ and modified $u-\phi$ formulations. This is elaborated in the following theorem.

Theorem 3
The poles of the $u-p$ formulation in (2)-(3) and the modified $u-\phi$ formulation in (16)-(17) are equal.

Proof
Consider the Laplace transform of the system equations (1)

$$\left(\mathbf{K}+s\mathbf{C}+s^2\mathbf{M}\right)\mathbf{X}(s)=\mathbf{F}(s).$$

The poles of the system are the values for s for which the matrix $\left(\mathbf{K}+s\mathbf{C}+s^2\mathbf{M}\right)$ becomes singular. Consequently, finding the poles of this system is equivalent to finding the values for s for which *det* $\left(\mathbf{K}+s\mathbf{C}+s^2\mathbf{M}\right)=0$. For the $u-p$ formulation (2)-(3) the poles are then given by

$$\begin{vmatrix}\mathbf{K_s}+s\mathbf{C_s}+s^2\mathbf{M_s} & \mathbf{K_c}\\ -\rho s^2\mathbf{K_c^T} & \mathbf{K_a}+s\mathbf{C_a}+s^2\mathbf{M_a}\end{vmatrix}=0.$$

For ease of notation we define $\mathbf{G}(s)\equiv\mathbf{K_s}+s\mathbf{C_s}+s^2\mathbf{M_s}$ and $\mathbf{H}(s)\equiv\mathbf{K_a}+s\mathbf{C_a}+s^2\mathbf{M_a}$. The previous equation then becomes

$$\begin{vmatrix}\mathbf{G}(s) & \mathbf{K_c}\\ -\rho s^2\mathbf{K_c^T} & \mathbf{H}(s)\end{vmatrix}=0. \tag{19}$$

For the modified $u-\phi$ formulation (16)-(17) we divide both sides of the set of equations governing the acoustic behaviour (the bottom set of equations) by ρ. The poles are then found as

$$\begin{vmatrix}\mathbf{K_s}+s\mathbf{C_s}+s^2\mathbf{M_s} & -s\rho\mathbf{K_c}\\ s\mathbf{K_c^T} & \mathbf{K_a}+s\mathbf{C_a}+s^2\mathbf{M_a}\end{vmatrix}=\begin{vmatrix}\mathbf{G}(s) & -s\rho\mathbf{K_c}\\ s\mathbf{K_c^T} & \mathbf{H}(s)\end{vmatrix}=0. \tag{20}$$

Since the determinants in (19) and (20) are equal, the poles of the two formulations are identical. □

Because these two formulations have identical poles, stability is preserved when converting a system from the $u-p$ formulation (2)-(3) to the modified $u-\phi$ formulation (16)-(17) and vice versa.

In order to apply theorem 3 to a vibro-acoustic system in $u-p$ formulation it is necessary that its system matrices have the same structure as in (3). This block-partitioned structure is present because the structural and acoustic degrees of freedom are separated. In general this structure is lost

DOI: 10.1002/nme

in the reduction process, and it is therefore not possible to convert the reduced $u-p$ system to an equivalent system in the modified $u-\phi$ formulation (or vice versa) after the reduction step. This is also the case for the stable reduced-order models obtained by the method proposed in section 5.1.

Let the standard projection basis $V \in \mathbb{C}^{n\times r}$, obtained through any one-sided projection-based MOR method (e.g. Krylov-subspace projection, modal truncation, ...), be given by

$$\mathbf{V} = \begin{bmatrix} \mathbf{V_s} \\ \mathbf{V_a} \end{bmatrix}. \tag{21}$$

with $V_s \in \mathbb{C}^{n_s\times r}$ the part of the projection matrix that corresponds to the structural degrees of freedom and $V_a \in \mathbb{C}^{n_a\times r}$ the part corresponding to the acoustic degrees of freedom. The projection of the vibro-acoustic system in the modified $u-\phi$ formulation (16)-(17) onto this basis $\mathbf{V}$ results in:

$$\mathbf{M_{mu\phi_r}}\ddot{\hat{\mathbf{x}}}_{\mathbf{u\phi}} + \mathbf{C_{mu\phi_r}}\dot{\hat{\mathbf{x}}}_{\mathbf{u\phi}} + \mathbf{K_{mu\phi_r}}\hat{\mathbf{x}}_{\mathbf{u\phi}} = \mathbf{F_{mu\phi_r}}, \tag{22}$$

with

$$\begin{aligned}
\mathbf{M_{mu\phi_r}} &= \mathbf{V^T M_{mu\phi} V} = \mathbf{V_s^T M_s V_s} + \rho \mathbf{V_a^T M_a V_a} \\
\mathbf{C_{mu\phi_r}} &= \mathbf{V^T C_{mu\phi} V} = \mathbf{V_s^T C_s V_s} + \rho \mathbf{V_a^T C_a V_a} - \rho \mathbf{V_s^T K_c V_a} + \rho \mathbf{V_a^T K_c^T V_s} \\
\mathbf{K_{mu\phi_r}} &= \mathbf{V^T K_{mu\phi} V} = \mathbf{V_s^T K_s V_s} + \rho \mathbf{V_a^T K_a V_a} \\
\mathbf{F_{mu\phi_r}} &= \mathbf{V^T F_{mu\phi}} = \mathbf{V_s^T F_s} + \mathbf{V_a^T F_\phi} \\
\hat{\mathbf{x}}_{\mathbf{u\phi}} &= \mathbf{V^{-1} x_{u\phi}}
\end{aligned} \tag{23}$$

These matrices no longer possess the block structure that was present in the original system matrices in (17) and can therefore not be converted back to an equivalent system in $u-p$ formulation. Note that the second-order structure of the system is preserved, and only the block structure *within* these second-order system matrices that corresponds to the structural-acoustic DOF separation is lost.

Using a projection basis with a carefully chosen structure however, we are able to retain the block structure within the second-order system matrices, thus allowing for conversion between the $u-p$ and modified $u-\phi$ formulation after the reduction step. This is achieved by augmenting the projection basis from (21) with zero blocks to obtain the extended projection basis $\tilde{\mathbf{V}}$:

$$\tilde{\mathbf{V}} = \begin{bmatrix} \mathbf{V_s} & \mathbf{0} \\ \mathbf{0} & \mathbf{V_a} \end{bmatrix}. \tag{24}$$

This strategy is similar to the one proposed in [33] to achieve block structure preserving MOR for coupled systems. Remark that the space spanned by the columns of $\tilde{\mathbf{V}}$ contains the space spanned by the columns of $\mathbf{V}$, such that when using $\tilde{\mathbf{V}}$ the reduced system will be *at least* as accurate as when using $\mathbf{V}$. For practical implementation it is recommended to orthogonalize $\tilde{\mathbf{V}}$, which equates to orthogonalizing both $\mathbf{V_s}$ and $\mathbf{V_a}$. Also note that $\tilde{\mathbf{V}}$ has twice as many columns as $\mathbf{V}$ such that the projected system will contain twice as many degrees of freedom (DOFs). Since $\mathbf{V_s}$ and $\mathbf{V_a}$ may be rank-deficient this can be slightly ameliorated by using a rank-revealing algorithm for the orthogonalization of $\mathbf{V_s}$ and $\mathbf{V_a}$, but to the authors' experience the total number of columns in $\tilde{\mathbf{V}}$ still remains close to twice the number of columns in $\mathbf{V}$. Projecting the system of equations (2)-(3) onto the extended basis $\tilde{\mathbf{V}}$ results in:

$$\mathbf{M_{upx_r}}\ddot{\hat{\mathbf{x}}}_{\mathbf{upx}} + \mathbf{C_{upx_r}}\dot{\hat{\mathbf{x}}}_{\mathbf{upx}} + \mathbf{K_{upx_r}}\hat{\mathbf{x}}_{\mathbf{upx}} = \mathbf{F_{upx_r}}, \tag{25}$$

with

DOI: 10.1002/nme

$$\mathbf{M_{upx_r}} = \begin{bmatrix} \mathbf{M_{s,r}} & \mathbf{0} \\ -\rho\mathbf{K_{c,r}^T} & \mathbf{M_{a,r}} \end{bmatrix} \qquad \mathbf{C_{upx_r}} = \begin{bmatrix} \mathbf{C_{s,r}} & \mathbf{0} \\ \mathbf{0} & \mathbf{C_{a,r}} \end{bmatrix} \qquad \mathbf{K_{upx_r}} = \begin{bmatrix} \mathbf{K_{s,r}} & \mathbf{K_{c,r}} \\ \mathbf{0} & \mathbf{K_{a,r}} \end{bmatrix}$$
$$\hat{\mathbf{x}}_{\mathbf{upx}} = \begin{bmatrix} \hat{\mathbf{u}} \\ \hat{\mathbf{p}} \end{bmatrix} \qquad \mathbf{F_{upx_r}} = \begin{bmatrix} \mathbf{F_{s,r}} \\ \mathbf{F_{a,r}} \end{bmatrix} \tag{26}$$

and

$$\begin{aligned} \mathbf{M_{s,r}} &= \mathbf{V_s^T M_s V_s} & \mathbf{M_{a,r}} &= \mathbf{V_a^T M_a V_a} \\ \mathbf{C_{s,r}} &= \mathbf{V_s^T C_s V_s} & \mathbf{C_{a,r}} &= \mathbf{V_a^T C_a V_a} \\ \mathbf{K_{s,r}} &= \mathbf{V_s^T K_s V_s} & \mathbf{K_{a,r}} &= \mathbf{V_a^T K_a V_a} \\ \hat{\mathbf{u}} &= \mathbf{V_s^{-1} u} & \hat{\mathbf{p}} &= \mathbf{V_a^{-1} p} \\ \mathbf{F_{s,r}} &= \mathbf{V_s^T F_s} & \mathbf{F_{a,r}} &= \mathbf{V_a^T F_a} \\ \mathbf{K_{c,r}} &= \mathbf{V_s^T K_c V_a}. \end{aligned}$$

By lemma 1 the matrices $\mathbf{M_{s,r}}$ and $\mathbf{M_{a,r}}$ are symmetric positive definite, $\mathbf{K_{s,r}}$ and $\mathbf{K_{a,r}}$ are symmetric positive (semi-)definite and $\mathbf{C_{s,r}}$ and $\mathbf{C_{a,r}}$ are positive (semi-) definite but not necessarily symmetric. This system of equations therefore has the same structure and properties as the unprojected system of equations in the standard $u-p$ formulation (2)-(3), and could therefore be converted to an equivalent modified $u-\phi$ formulation as in (16). The same reduced system in the modified $u-\phi$ formulation could also have been obtained in an alternative way, namely by projecting the modified $u-\phi$ representation of the full, unreduced system onto the basis $\tilde{\mathbf{V}}$. Such a one-sided projection has already been shown to retain stability. Because the equivalent reduced system in the modified $u-\phi$ formulation is stable, theorem 3 implies that its $u-p$ counterpart in (25)-(26) is also stable. In other words: the stability of a system in $u-p$ formulation is preserved in a one-sided projection onto a basis with the structure of $\tilde{\mathbf{V}}$ as in (24).

The structural and acoustic degrees of freedom remain segregated in the reduced-order model with this method. This holds the additional benefit that staggered time integration schemes can be used, where the structural and fluid portions of the problem are integrated separately (and possibly in parallel) [34–36]. This is not possible for the method developed in section 5.1. The use of a staggered integration scheme with parallel implementation may be able to compensate for the disadvantage of the increased system size of the ROM in (25) compared to the ROM in (22). In this regard it is interesting to note that the reduced structural and acoustic subdomains in (26) each have a size that is comparable to the size of the ROM in (22).

It is possible to use any one-sided projection-based MOR method for second-order systems to generate a projection basis $\mathbf{V}$ as in (21) and then split and augment this basis to obtain $\tilde{\mathbf{V}}$ in (24). Alternatively some MOR techniques exist that immediately produce a projection matrix which has the structure of $\tilde{\mathbf{V}}$. Substructuring techniques such as component mode synthesis (CMS) are a popular choice of MOR method for vibro-acoustic systems, often paired to a finite element model in $u-p$ formulation [33, 37, 38]. The structural and acoustic domains are then considered as two separate "components" of the full coupled system and individual projection bases are constructed for each of these domains, which leads to a global projection matrix with the same structure as $\tilde{\mathbf{V}}$. The insights gained in this section allow us to prove that these methods are in fact stability-preserving.

In order to avoid ambiguity we wish emphasize that the partitioning of the projection matrix $\tilde{\mathbf{V}}$ in (24) is different from the split basis that is used in (13), and both are actually combined in the proposed method. The specific composition of $\mathbf{V_d}$ in (13) allows us to use MOR techniques that preserve the second-order structure of the problem. The extended projection matrix $\tilde{\mathbf{V}}$ in (24)

DOI: 10.1002/nme

is used to preserve the block structure *within* these second-order system matrices, which enables stability preservation.

5.3. Limitations of the proposed methods

In this section two novel techniques for stability preserving MOR of coupled vibro-acoustic FE models were proposed. The first technique arranges the system into the modified $u - \phi$ formulation of (16), after which any one-sided projection is guaranteed to preserve stability. The second method uses an extended one-sided projection basis $\tilde{\mathbf{V}}$ to ensure preservation of stability, which implies that the system can also be left in the more commonly used $u - p$ formulation.

The original system has to meet certain requirements in order for the proposed techniques to be applicable:

- The system matrices are frequency-independent.
- The matrices $\mathbf{K_s}$ and $\mathbf{K_a}$ are symmetric positive (semi-)definite.
- The matrices $\mathbf{M_s}$ and $\mathbf{M_a}$ are symmetric positive definite.
- The matrices $\mathbf{C_s}$ and $\mathbf{C_a}$ are positive (semi-)definite, but not necessarily symmetric.
- The projection matrix $\mathbf{V}$ can be any complex $n \times r$ matrix, as long as it is of rank r.

6. WORKFLOW

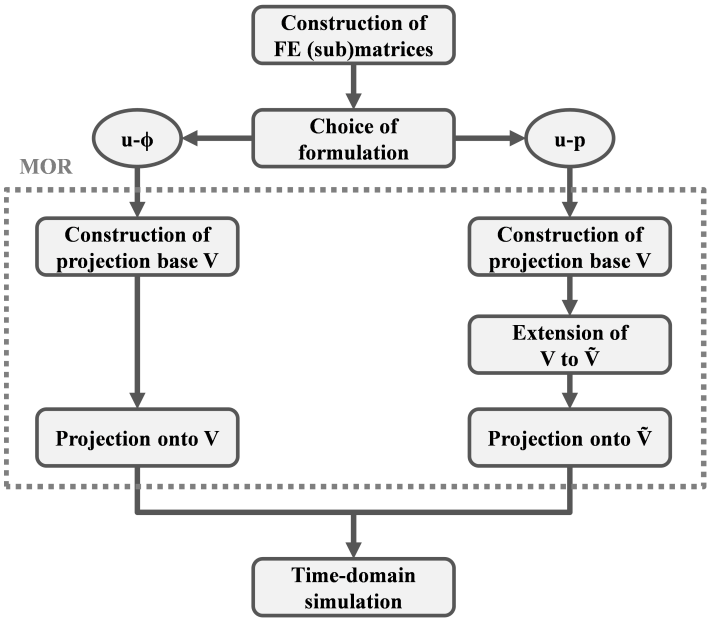

Figure 1. Workflow of the proposed method.

This section condenses the findings from the preceding sections into a structured workflow for performing efficient time-domain simulation of vibro-acoustic FE models using stability-preserving MOR. A schematic of this workflow is depicted in figure 1.

The first step consists of constructing the system (sub)matrices $\mathbf{M_s}, \mathbf{C_s}, \mathbf{K_s}, \mathbf{M_a}, \mathbf{C_a}, \mathbf{K_a}$ and $\mathbf{K_c}$ of the vibro-acoustic FE model. Once these have been obtained, the next step comprises the choice of formulation. This is achieved by assembling the global system matrices either as in the

DOI: 10.1002/nme

common $u-p$ formulation in (2)-(3) or the modified $u-\phi$ formulation in (16)-(17). The branch of the workflow that is followed in figure 1 depends on this choice of formulation.

In case the modified $u-\phi$ formulation is chosen the MOR is performed in a conventional way: a projection basis $\mathbf{V}$ is constructed using any one-sided MOR method, after which a stable ROM is obtained by projecting the system matrices onto this basis as in (22)-(23). If, on the other hand, the $u-p$ formulation is chosen, it becomes necessary to extend the projection basis $\mathbf{V}$ to $\tilde{\mathbf{V}}$ as in (24) to ensure the stability of the projected system. The projection of the system matrices on this extended basis $\tilde{\mathbf{V}}$ is then performed according to (25)-(26).

Now that we have a stable ROM, either in the $u-p$ or the modified $u-\phi$ formulation, it becomes possible to perform accurate time-domain simulations efficiently using any time-integration method suitable for first- or second-order systems. Staggered integration schemes where the structural and fluid partitions of the problem are integrated separately can only be used with a split projection basis $\tilde{\mathbf{V}}$.

Note that it is advisable to use the modified $u-\phi$ formulation for stability-preserving MOR of coupled vibro-acoustic FE models. Keeping the system in $u-p$ formulation necessitates the use of an extended projection basis $\tilde{\mathbf{V}}$, resulting in a reduced-order model with possibly up to twice as many DOFs.

7. NUMERICAL EXPERIMENTS

This section demonstrates the advantages of the proposed methods for time-domain simulation of reduced-order vibro-acoustic models. Two cases are studied: the first case consists of a square aluminium panel backed by a cube-shaped cavity with sound hard boundaries while the second case tackles a more complex car interior geometry with vibrating roof and normal impedance boundary condition on the seats. The first case is an academical example which is reproducible and therefore serves as a benchmark problem. The second case demonstrates that the proposed techniques are effective when applied to problems of industrial size and complexity.

7.1. Cube-shaped cavity with square aluminium plate

The vibro-acoustic system used in this analysis consists of a square, cavity-backed aluminium plate, discretized by the finite element method with linear elements. The element size is chosen such that a resolution of at least 6 elements per wavelength is obtained at 500 Hz. The cavity geometry is a cube with an edge length of 1m. The plate has an edge length of 1m and is 3mm thick. The plate is clamped at its edges and is modeled using shell-type elements. The acoustic cavity is filled with air, and the enclosing walls are rigid. The excitation consists of a point force acting on the plate located at (0.2, 0.32, 1) m, and the sound pressure is calculated at (0.76, 0.6, 0.2) m. Figure 2 shows a graphical representation of this system, and table I lists the material properties.

In this analysis, we compare the properties and performance of a conventional reduced-order model in $u-p$ formulation *not* using an extended projection basis, a reduced-order model in $u-p$ formulation *with* an extended projection basis, a reduced-order model using the *standard* $u-\phi$ formulation and a reduced-order model obtained using the *modified* $u-\phi$ formulation. The original full-order finite element model consists of 20456 DOFs, 2880 of which correspond to the plate and 17576 to the acoustic cavity. The damping included in this system was modeled as Rayleigh damping ($\mathbf{C_s} = \alpha\mathbf{M_s} + \beta\mathbf{K_s}$ and $\mathbf{C_a} = \alpha\mathbf{M_a} + \beta\mathbf{K_a}$). For the reduced-order models, the projection basis is constructed using a one-sided second-order Arnoldi process where the expansion points are determined by an iterative procedure, resulting in a reduced-order model with a total of 123 DOFs [29, 39]. The reduced-order model obtained with the extended projection basis and the $u-p$ formulation has 245 DOFs, which is almost twice as much as with the non-extended

DOI: 10.1002/nme

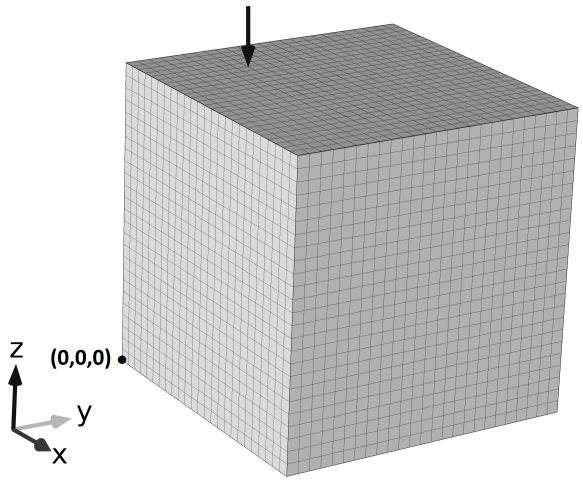

Figure 2. Geometry and finite element mesh of the cube-shaped cavity with square aluminium plate.[‡]

projection basis. To assess the quality of approximation of the reduced-order models, we first look at the frequency response function (FRF) of the acoustic pressure to the point force excitation. Figure 3 displays the FRFs obtained with the full FE model and all of the reduced-order models. Figure 4 depicts the relative error on the amplitude of the FRFs obtained with these reduced models. The relative error is defined as

$$\varepsilon = \frac{|FRF_{\text{ROM}} - FRF_{\text{full FE}}|}{|FRF_{\text{full FE}}|}.$$

The expansion points and Krylov subspace orders used to construct the projection bases are identical for all formulations, thus allowing for a fair comparison. Keep in mind however that the model obtained by projection of the system in $u-p$ formulation on the extended basis $\tilde{\mathbf{V}}$ is larger in size than the others. As these figures show, the ROMs match the behaviour of the full FE model up to a frequency of approximately 400 Hz. The frequency range in which the original model behaviour is matched by the reduced-order models is determined by the choice of expansion points and Krylov subspace orders [40]. In this sense there is a trade-off between ROM size and the width of the frequency range in which the ROM is an accurate representation of the full-order model: It is possible to extend the frequency range in which the ROMs are accurate but this will increase the number of DOFs in the ROMs.

The error plot in figure 4 also shows that of the two reduced-order models in $u-p$ formulation, the model obtained with the extended basis is consistently more accurate than the one obtained with the non-extended basis. This confirms the statement we made regarding the column spaces of $\mathbf{V}$ and $\tilde{\mathbf{V}}$ in section 5.2.

Although all of these methods can be used to obtain an accurate reduced-order model for frequency-domain analysis, we additionally require preservation of stability to accurately match time-domain behaviour. Figure 5 shows that both the reduced $u-p$ model using a non-extended projection basis and the reduced model using a standard $u-\phi$ formulation have poles in the right-half of the complex plane, indicating instability. A closer look at the poles of the reduced model in $u-p$ formulation with extended basis and the one in the modified $u-\phi$ formulation

[‡]The FE model and corresponding figure were generated using COMSOL Multiphysics 5.0

DOI: 10.1002/nme

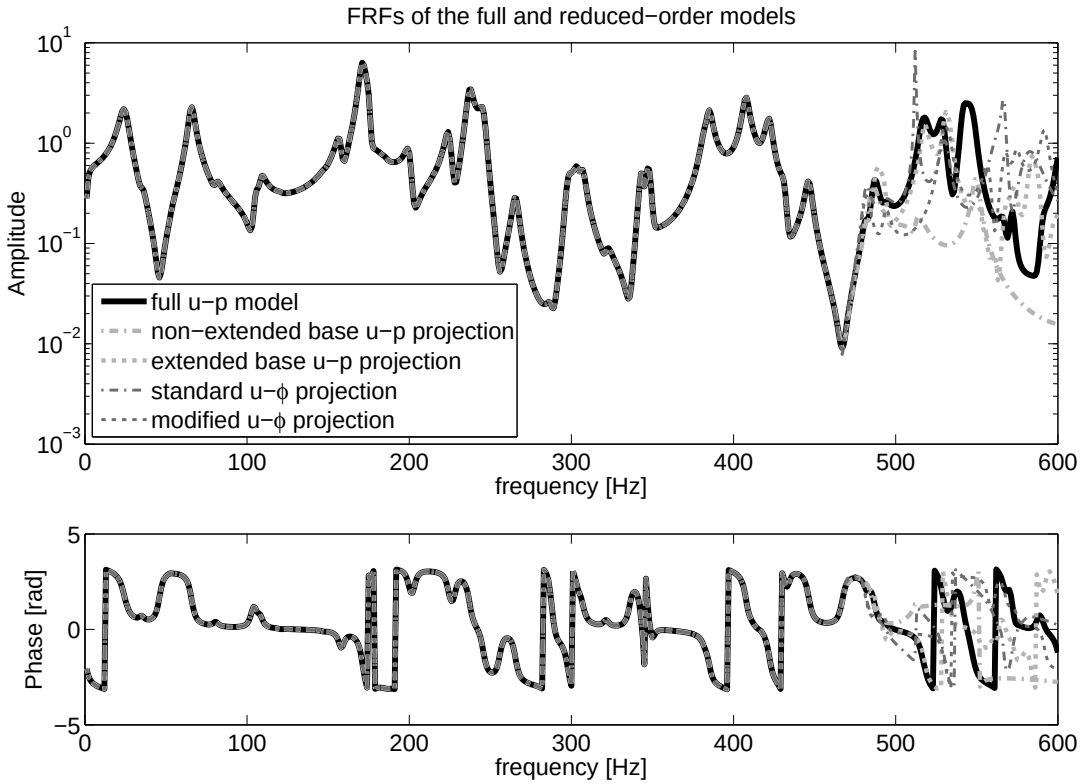

Figure 3. The FRFs of the reduced-order models approximate the FRF of the full FE model of the cube-shaped cavity well up to about 400 Hz.

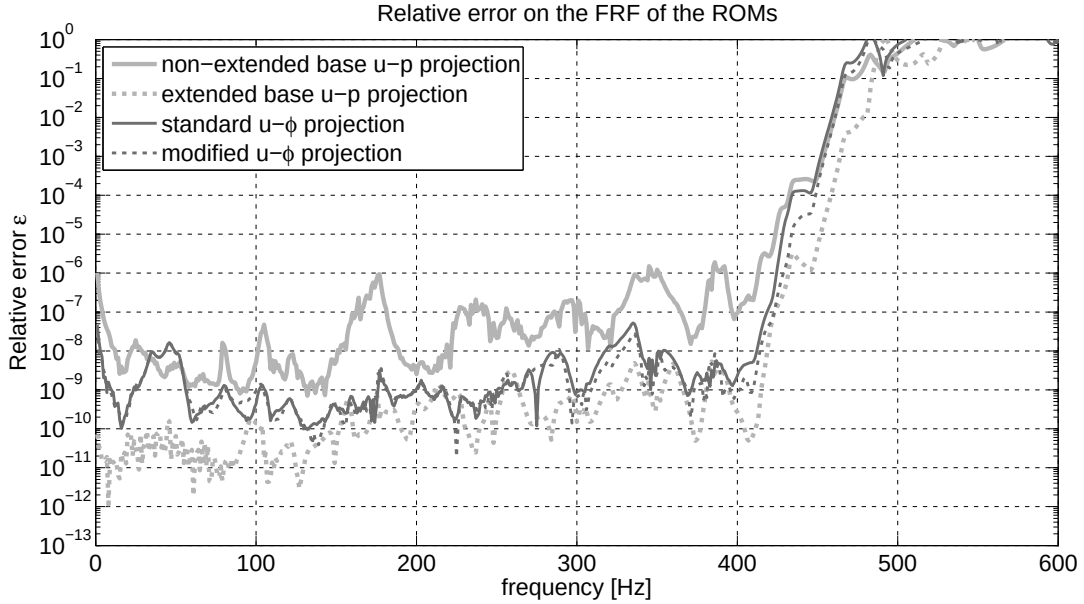

Figure 4. The reduced-order models exhibit a small relative error on the FRF amplitude up to 400 Hz. Extending the projection basis $\mathbf{V}$ to $\tilde{\mathbf{V}}$ increases the accuracy of the reduced-order model in the $u-p$ formulation.

DOI: 10.1002/nme

reveals that they are all in the left-half of the complex plane; the stability of the original FE model has been preserved in the projection. Note that there is a pole at the origin of the complex plane, indicating the existence a rigid-body mode. This rigid-body mode corresponds to a uniform pressure variation of the acoustic fluid. Figure 6 shows a close-up of the poles of the stable reduced-order models (the modified $u-\phi$ projection and the $u-p$ projection with an extended basis) and the full-order model. It can be seen that the poles of the stable reduced-order models approximate the poles of the original system very well up to about 400 Hz ($\simeq$ 2500 rad/s). This is in agreement with our previous observation concerning the approximation accuracy in the frequency-domain.

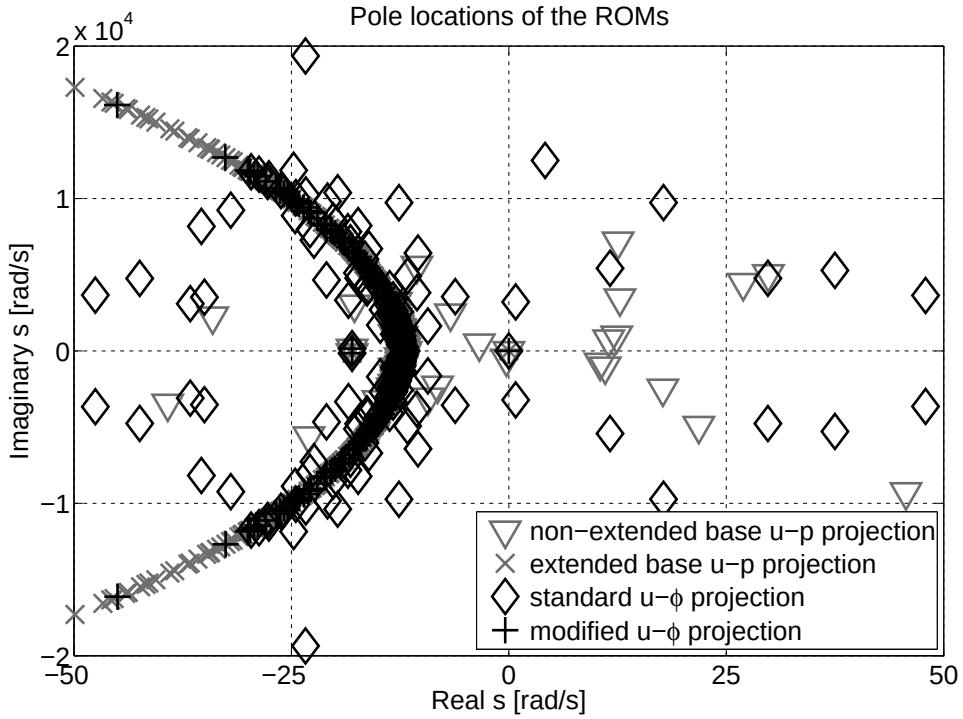

Figure 5. The reduced $u-p$ model without extended basis and the reduced model in standard $u-\phi$ formulation have poles in the right-half of the complex s-plane, indicating instability.

The use of the extended projection basis increases the ROM size but also enhances the accuracy, making it difficult to judge its performance compared to the other reduction methods. A good assessment of the relative performance of the different reduction methods can be made by means of a convergence study. To this end figure 7 shows how the $\mathcal{H}_2$-norm of the relative FRF amplitude error ε (evaluated over the range of 1 to 400 Hz) evolves with increasing ROM size. It can be observed that the method using an extended projection basis is unable to match the accuracy of the other methods for a given ROM size, or conversely that it requires more reduced DOFs to achieve a similar accuracy.

The time responses of the reduced $u-p$ model with non-extended basis and the reduced model in standard $u-\phi$ formulation are almost instantly dominated by the exponentially growing contributions of the unstable poles, which makes these systems infeasible for analysis in the time-domain. In contrast, the reduced models generated using the modified $u-\phi$ formulation or using an extended projection basis are perfectly suitable for time integration. Note that, since the reduced model only matches the full system behaviour up to 400 Hz, it will only be accurate in the time-domain for the part of the response that falls within this spectrum. Figure 8 presents the time responses of the full FE model, the reduced $u-\phi$ model and the reduced $u-p$ model with extended basis. The input force is a sine of which the frequency varies linearly in time. The

DOI: 10.1002/nme

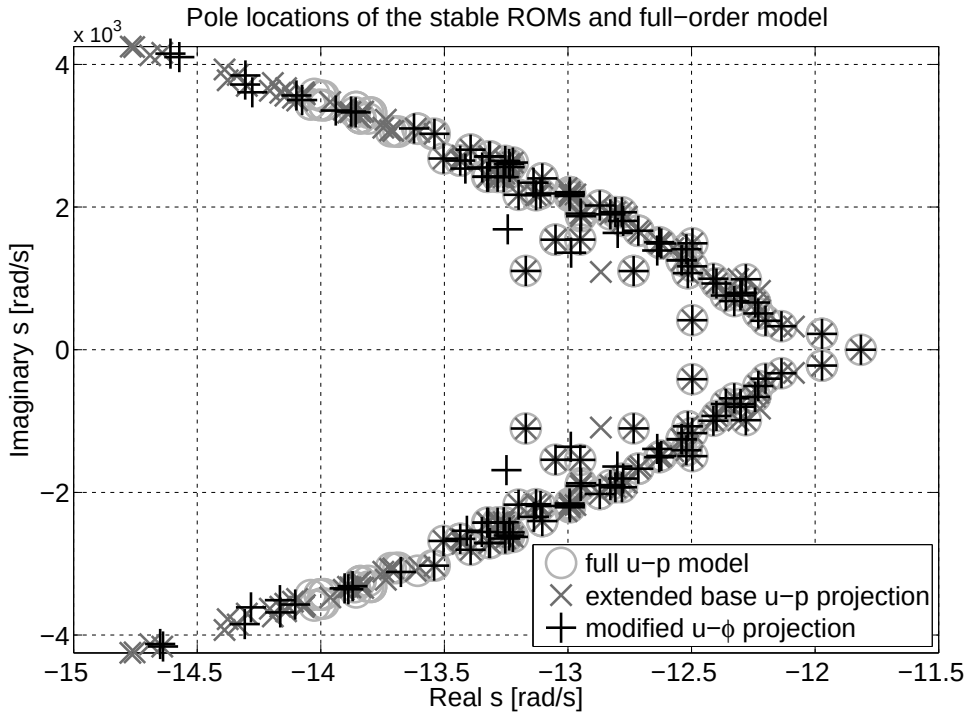

Figure 6. The poles of the full model and the stable reduced-order models of the cube-shaped cavity match well up to about 400 Hz ($\simeq$ 2500 rad/s).

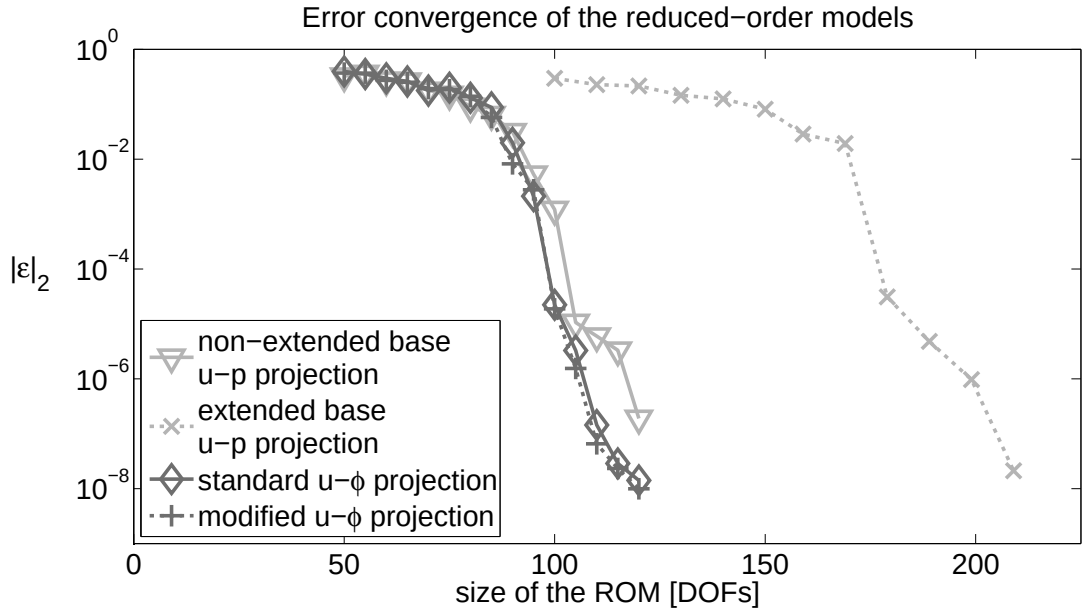

Figure 7. The extended base $u-p$ projection method is less efficient than the other reduction methods in terms of accuracy per DOF.

frequency sweeps up from 0 to 400 Hz in the first second of the simulation. Then it sweeps back down again to 0 Hz at 2s. The simulation was performed using a generalized-α time integration scheme without numerical dissipation and with a time step of $1,25.10^{-4}$ s, which is sufficiently small with respect to the frequency range of interest [41]. As can be seen from the figure, the

DOI: 10.1002/nme

error introduced by the model reduction is extremely small. The strong reduction in model size accomplished by the projection-based MOR leads to a significant reduction in computational effort while still retaining model accuracy.

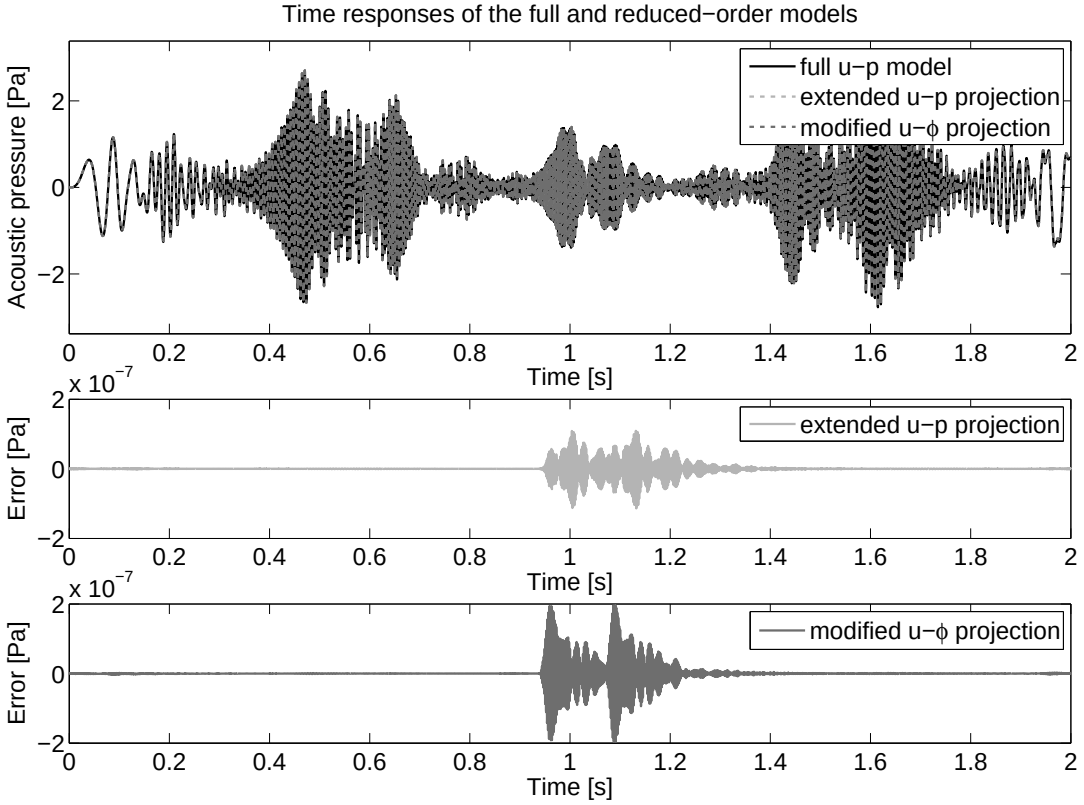

Figure 8. The extended $u-p$ and modified $u-\phi$ reduced models accurately describe the time-domain behaviour of the full FE model of the cube-shaped cavity.

7.2. Car interior with vibrating roof and normal impedance

For the second case we study the vibro-acoustic behaviour of a car interior, the geometry of which is shown in figure 9a. This example demonstrates that the developed methods are not confined to geometrically simple cases and can handle problems of industrial size and complexity. The roof of the car is modeled as a flexible steel panel with a thickness of 2 mm which is clamped at its boundaries and the interior is filled with air. Elements with linear shape functions are used with an element size that provides a resolution of at least 6 elements per wavelength up to 200 Hz. The resulting finite element mesh is depicted in figure 9b. The mesh is finer near the plate than in the bulk of the fluid since the wavelength of the bending waves in the structure is smaller than the acoustic wavelength at 200 Hz. A normal impedance boundary condition is imposed on the seat surfaces to represent the properties of the fabric. The normal impedance value is chosen to be two times the characteristic impedance of air. All the other boundaries of the acoustic domain are considered to behave as rigid walls. The damping in the structure is again modeled as Rayleigh damping ($\mathbf{C_s} = \alpha\mathbf{M_s} + \beta\mathbf{K_s}$). Figure 10 shows which part of the geometry is modeled as shells and for which surfaces the normal impedance boundary condition applies. The excitation consists of a point force acting on the roof at (1.50 0.08 1.09) m, and the sound pressure is calculated at (0.73 0.23 0.68) m. Table II lists the material properties of the system.

DOI: 10.1002/nme

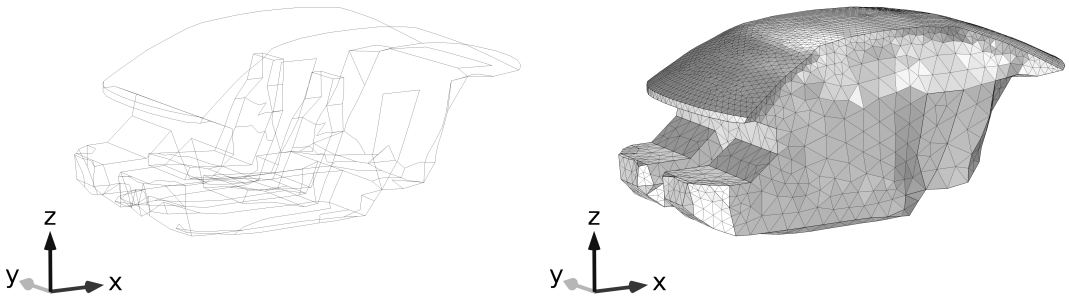

(a) Car interior geometry.‡ (b) Finite element mesh for the car interior geometry.‡

Figure 9. Geometry of the model and finite element mesh.

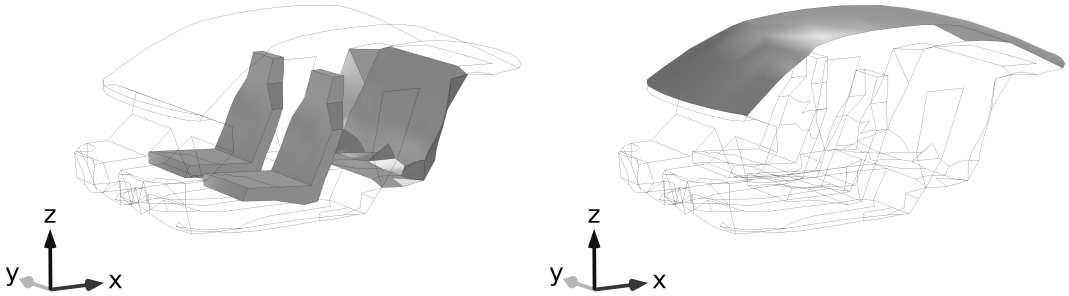

(a) Surfaces with implied normal impedance.‡ (b) The structural part modeled with shells.‡

Figure 10. Boundary conditions and structural part of the model.

The finite element model of the roof and car interior has 14038 DOFs in total. The roof of the car accounts for 7455 structural DOFs and the acoustic cavity for 6583 DOFs. The model order reduction technique that is used is again a one-sided Krylov subspace projection where the projection basis is constructed using the second-order Arnoldi algorithm [29, 39]. The expansion points are determined through an iterative procedure. With the exception of the $u-p$ projection with extended basis, all the reduced-order models consist of 60 DOFs. The use of the extended basis $\tilde{\mathbf{V}}$ as in (21) however results in a reduced-order model with a size of 120 DOFs.

As can be seen in figures 11 and 12 all of the studied model order reduction techniques are able to accurately describe the full system behaviour in the frequency-domain up to about 200 Hz. As expected the $u-p$ projected system with the extended basis is more accurate than the reduced-order model that is obtained with the non-extended basis. The frequency up to which the reduced-order models accurately approximate the full-order model can be increased by using additional expansion points to calculate the Krylov subspace but this would also enlarge the reduced-order model size.

Similar to the previous numerical experiment both the $u-p$ projection without extended basis and the projection of the system in standard $u-\phi$ formulation lead to unstable reduced-order models. This is shown in figure 13 as these models have poles in the right-half of the complex plane. The comparison of the pole locations of the full-order model, the $u-p$ projection with extended basis and the projection of the system in the modified $u-\phi$ formulation in figure 14 shows that these stable reduced-order models accurately approximate the poles of the full-order model up to about 200 Hz ($\simeq$ 1250 rad/s).

DOI: 10.1002/nme

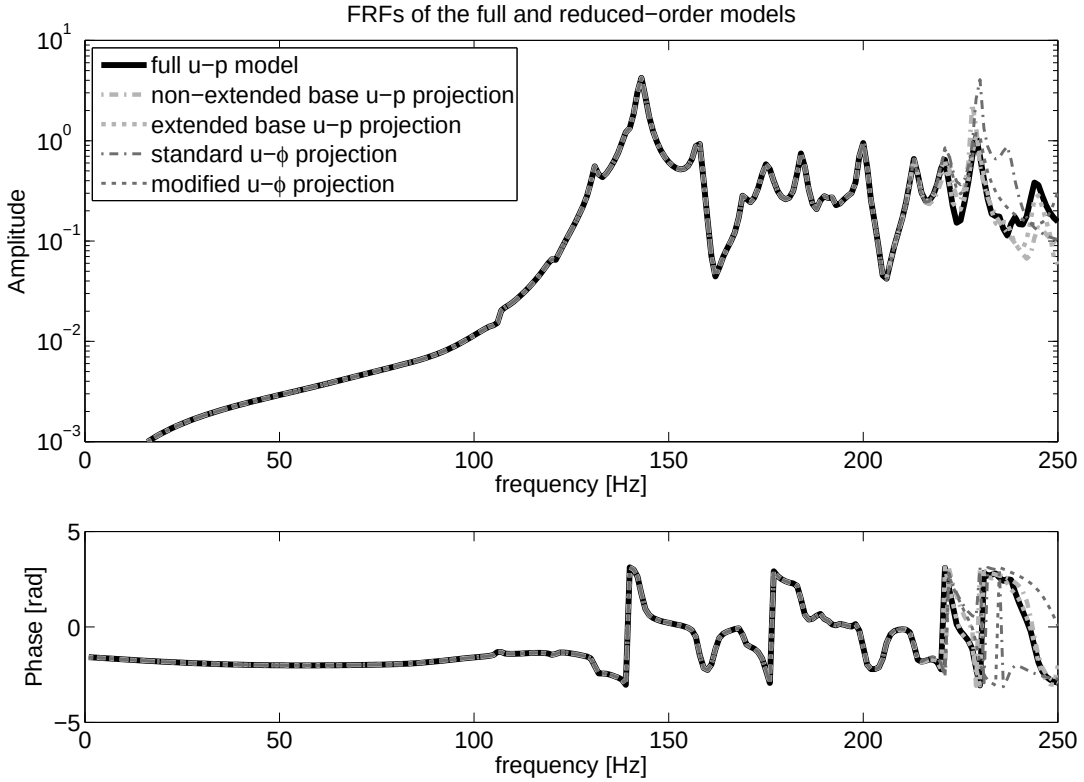

Figure 11. The studied reduced-order models approximate the FRF of the full-order model well up to about 200 Hz for the car cavity model.

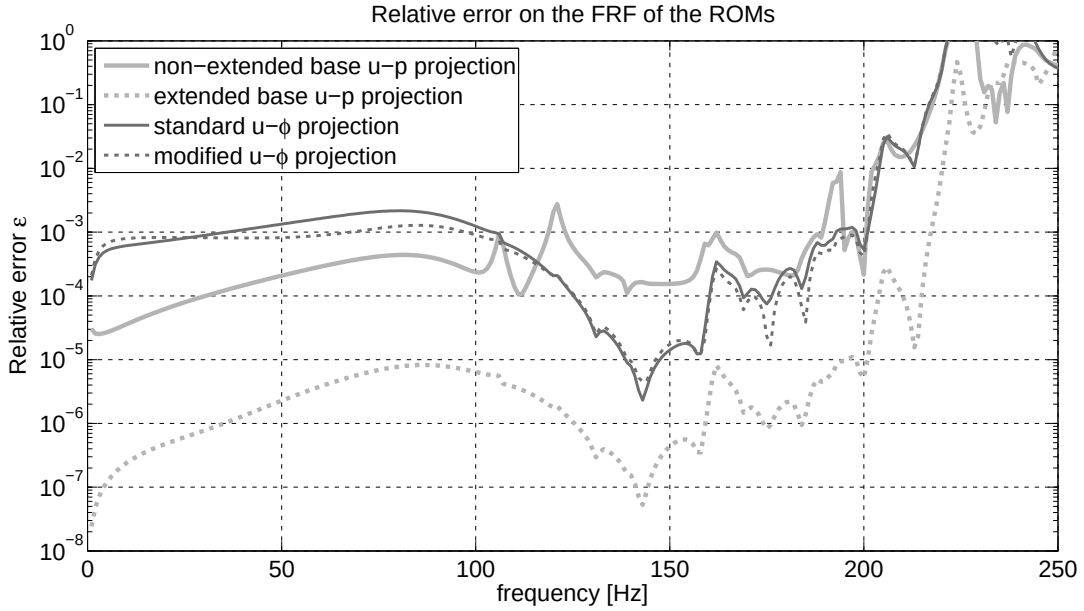

Figure 12. The reduced-order models of the car cavity exhibit a small error on the FRF amplitude up to about 200 Hz.

DOI: 10.1002/nme

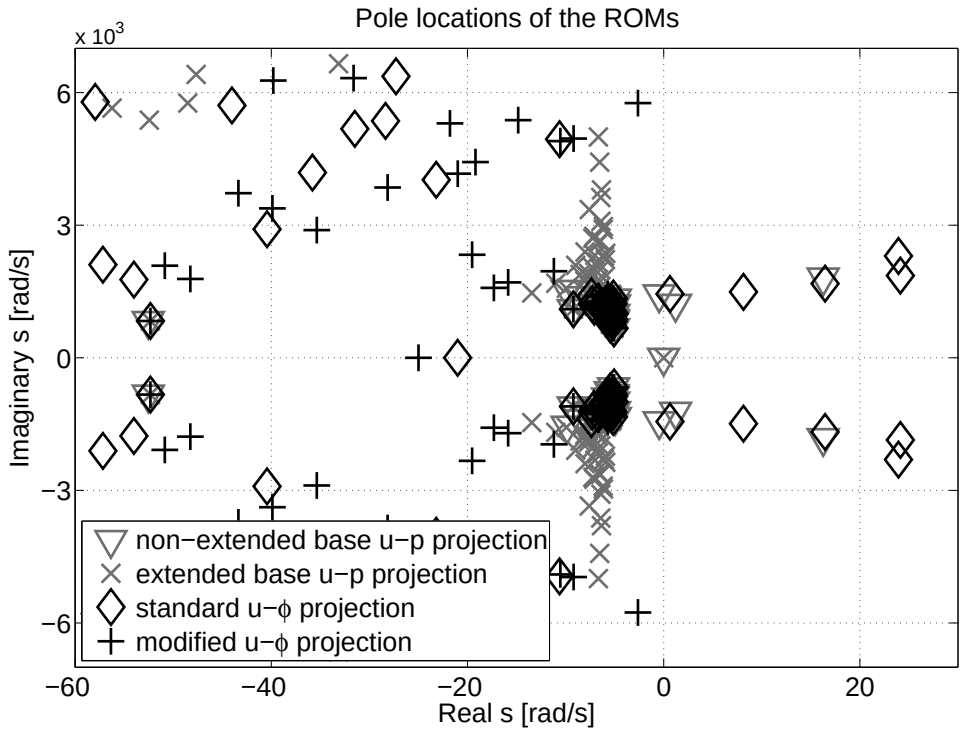

Figure 13. Pole locations of the reduced-order models of the car cavity. The non-extended basis $u - p$ projection and standard $u - \phi$ projection have poles in the right half-plane, indicating instability.

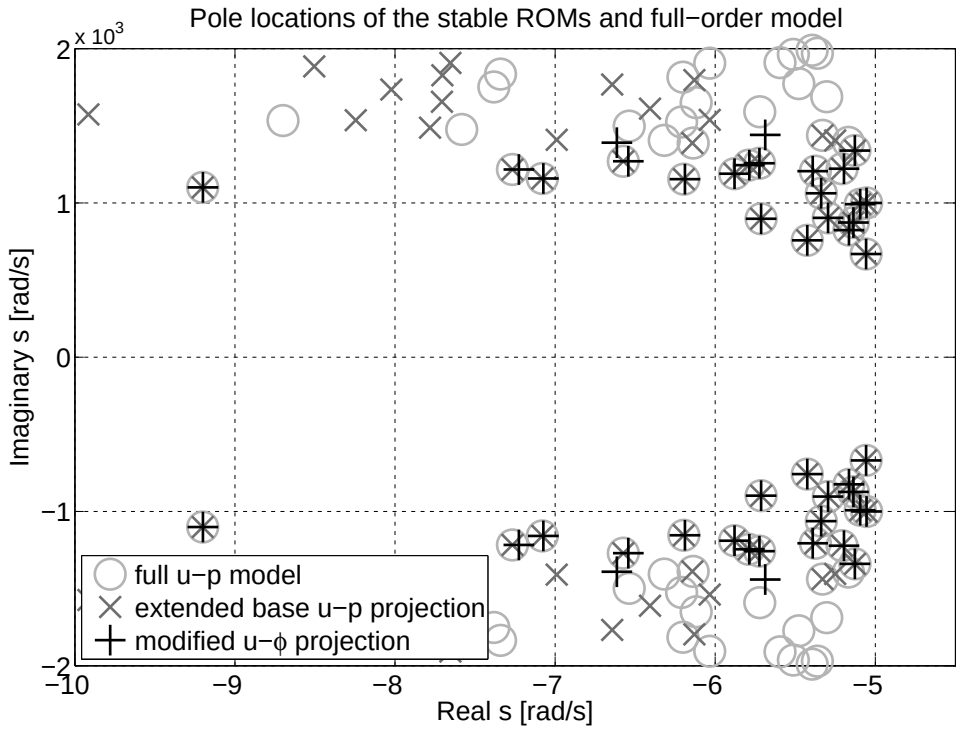

Figure 14. The poles of the stable reduced-order models match the poles of the original model of the car cavity well up to about 200 Hz ($\simeq$ 1250 rad/s).

DOI: 10.1002/nme

The convergence of the $\mathcal{H}_2$-norm of the relative FRF amplitude error ε was studied to compare the relative performance of the different reduction methods for this case study. The $\mathcal{H}_2$-norm of ε is evaluated over the range of 1 to 200 Hz. Figure 15 presents an overview of the results of this convergence study. Again the method using an extended projection basis performs substantially worse than the other methods when comparing them in terms of accuracy per DOF.

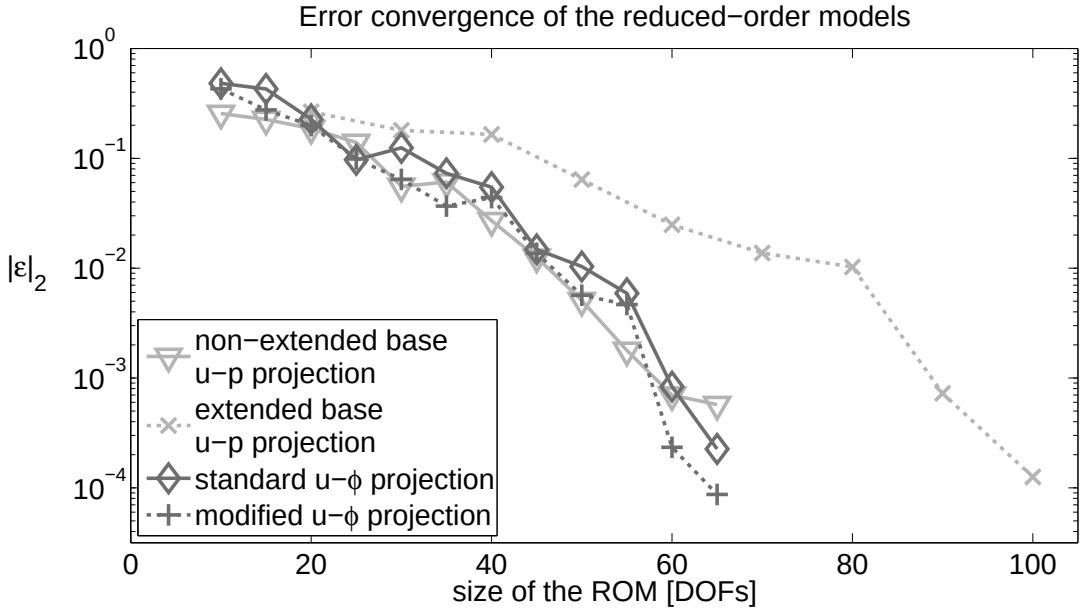

Figure 15. The extended base $u-p$ projection method is less efficient than the other reduction methods in terms of accuracy per DOF.

As a final test to assess the accuracy of the stable reduced-order models a time-domain simulation is performed with a swept sine force input. The frequency sweeps up from 0 to 200 Hz in the first second of the simulation after which it sweeps back down again to 0 Hz at 2s. This simulation was performed using a generalized-α time integration scheme without numerical dissipation and with a time step of $2,5.10^{-4}$ s, which is sufficiently small with respect to the frequency range of interest [41]. Figure 16 shows that also for this more complex case the proposed methods are able to provide a stable, efficient and accurate tool for the time-domain simulation of coupled vibro-acoustic finite element models.

DOI: 10.1002/nme

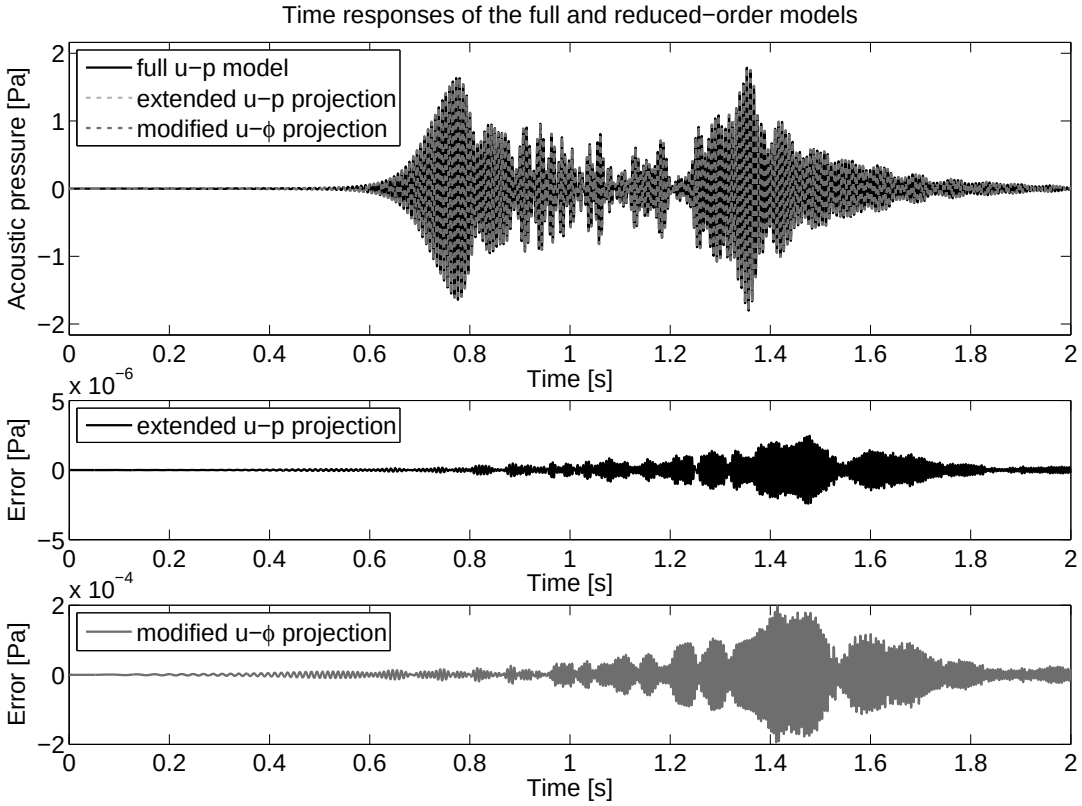

Figure 16. Time response and errors of the full and stable reduced-order models of the car cavity.

8. CONCLUSIONS

Two different frameworks for stability-preserving model order reduction in vibro-acoustics are proposed in this work. Starting from the theoretical study and proof of sufficient conditions for stability preservation in a one-sided projection, we design two methods that guarantee stability preservation for reduced vibro-acoustic models.

The first approach alters the displacement-fluid velocity potential ($u - \phi$) formulation such that it loses its symmetric nature in favor of a structure which preserves stability in a one-sided projection. The practice of adjusting the structure of the original model to obtain specific properties resulting in a stable reduced model is an original approach which has not been presented in literature before.

The second approach is based on a regular displacement-pressure ($u - p$) formulation and requires the projection space to be decoupled for the structural and acoustic domains in order to preserve stability. This method acts upon the projection space instead of the original model to achieve stability-preserving model order reduction.

The presented techniques are validated numerically in order to demonstrate their suitability for applications like time-domain simulation. The validation cases clearly show the shortcomings of classically reduced order models due to their unstable behavior and demonstrate the stable time-domain behavior of the newly presented approaches. The reduction of the introduced modified $u - \phi$ formulation provides the highest reduction efficiency, at the cost of a non-standard model description. The second approach allows for the system to be modeled in the common $u - p$ formulation, but requires an increase in ROM size to obtain similar accuracy.

ACKNOWLEDGEMENTS

The research of Axel van de Walle is funded by a Ph.D. Grant of the Agency for Innovation by Science

DOI: 10.1002/nme

and Technology in Flanders (IWT). The Fund for Scientific Research - Flanders (F.W.O.) is gratefully acknowledged for the support of the postdoctoral research of Frank Naets and Elke Deckers. The Industrial Research Fund KU Leuven is gratefully acknowledged for its support.

REFERENCES

[1] Chappell D, Harris P, Henwood D, Chakrabarti R. Modelling the transient interaction of a thin elastic shell with an exterior acoustic field. *International Journal for Numerical Methods in Engineering* 2008; **75**:275–290.

[2] Okuzono T, Otsuru T, Tomiku R, Okamoto N. Application of modified integration rule to time-domain finite-element acoustic simulation of rooms. *J. Acoustic. Soc. Am.* 2012; **132**:804–813.

[3] Mehra R, Raghuvanshi N, Savioja L, Lin M, Manocha D. An efficient GPU-based time domain solver for the acoustic wave equation. *Applied Acoustics* 2012; **73**:83–94.

[4] Bi C, Geng L, Zhang X. Cubic spline interpolation-based time-domain equivalent source method for modeling transient acoustic radiation. *Journal of Sound and Vibration* 2013; **332**:5939–5952.

[5] Okuzono T, Otsuru T, Tomiku R, Okamoto N. A finite-element method using dispersion reduced spline elements for room acoustics simulation. *Applied Acoustics* 2014; **79**:1–8.

[6] Hasheminejad S, Mousavi-Akbarzadeh H. Transient acoustic radiation from an eccentric sphere. *Applied Mathematical Modelling* 2015; **39**:5033–5046.

[7] Jog C, Nandy A. Conservation Properties of the Trapezoidal Rule in Linear Time Domain Analysis of Acoustics and Structures. *Journal of Vibration and Acoustics* 2015; **137**:021 010–021 010–17.

[8] Zienkiewicz O, Taylor R, Zhu J. *The Finite Element Method: Its Basis and Fundamentals*. Elsevier Science, 2005.

[9] Everstine G. Finite element formulations of structural acoustic problems. *Computers and Structures* 1997; **65**:307–321.

[10] Puri R, Morrey D, Bell A, Durodola J, Rudnyi E, Korvink J. Reduced order fully coupled structural–acoustic analysis via implicit moment matching. *Applied Mathematical Modelling* 2009; **33**:4097–4119.

[11] Marburg S. Six boundary elements per wavelength: is that enough? *Journal of Computational Acoustics* 2002; **10**:25–51.

[12] Antoulas A. *Approximation of Large-Scale Dynamical Systems (Advances in Design and Control)*. Society for Industrial and Applied Mathematics: Philadelphia, PA, USA, 2005.

[13] Herrmann J, Maess M, Gaul L. Substructuring including interface reduction for the efficient vibro-acoustic simulation of fluid-filled piping systems. *Mechanical Systems and Signal Processing* 2010; **24**:153–163.

[14] Hetmaniuk U, Tezaur R, Farhat C. Review and assessment of interpolatory model order reduction methods for frequency response structural dynamics and acoustics problems. *International Journal for Numerical Methods in Engineering* 2012; **90**:1636–1662.

[15] Moore B. Principal component analysis in linear systems: Controllability, observability, and model reduction. *IEEE Transactions on Automatic Control* 1981; **26**:17–32.

[16] Amsallem D, Farhat C. Stabilization of projection-based reduced-order models. *International Journal for Numerical Methods in Engineering* 2012; **91**:358–377.

[17] Bond B, Daniel L. Guaranteed Stable Projection-Based Model Reduction for Indefinite and Unstable Linear Systems. *Proceedings of the 2008 IEEE/ACM International Conference on Computer-Aided Design, San Jose, California, USA*, 2008; 728–735.

[18] Kalashnikova I, van Bloemen Waanders B, Arunajatesan S, Barone M. Stabilization of projection-based reduced order models for linear time-invariant systems via optimization-based eigenvalue reassignment. *Computer Methods in Applied Mechanics and Engineering* 2014; **272**:251–270.

DOI: 10.1002/nme

[19] Odabasioglu A, Celik M, Pileggi L. PRIMA: Passive Reduced-Order Interconnect Macromodelling Algorithm. *IEEE Transactions on Computer-Aided Design of Integrated Circuits and Systems* 1998; **17**(8):645–654.

[20] Silveira L, Kamon M, Elfadel I, White J. A Coordinate-Transformed Arnoldi Algorithm for Generating Guaranteed Stable Reduced-Order Models of RLC Circuits. *Proc. ICCAD*, 1996; 228–294.

[21] Sorensen D. Passivity preserving model reduction via interpolation of spectral zeros. *Systems and Control Letters* 2005; **54**:347–360.

[22] Antoulas A. A new result on passivity preserving model reduction. *Systems and Control Letters* 2005; **54**:361–374.

[23] Ionutiu R, Rommes J, Antoulas A. Passivity-Preserving Model Reduction Using Dominant Spectral-Zero Interpolation. *IEEE Transactions on Computer-Aided Design of Integrated Circuits and Systems* 2008; **27**(12):2250–2263.

[24] Everstine G. A symmetric potential formulation for fluid-structure interaction. Letter to the editor. *Journal of Sound and Vibration* 1981; **79**:157–160.

[25] Benner P, Mehrmann V, Sorensen D. *Dimension Reduction of Large-Scale Systems*. Springer, 2003.

[26] Chahlaoui Y, Gallivan K, Vandendorpe A, Van Dooren P. Model Reduction of Second-Order Systems. *Dimension Reduction of Large-Scale Systems*, Benner P, Mehrmann V, Sorensen D (eds.). Springer, 2003; 149–172.

[27] Bai Z, Meerbergen K, Su Y. Arnoldi Methods for Structure-Preserving Dimension Reduction of Second-Order Dynamical Systems. *Dimension Reduction of Large-Scale Systems*, Benner P, Mehrmann V, Sorensen D (eds.). Springer, 2003; 173–189.

[28] Amsallem D, Hetmaniuk U. Error estimates for Galerkin reduced-order models of the semi-discrete wave equation. *ESAIM: Mathematical Modelling and Numerical Analysis* 2013; **48**:135–163.

[29] Bai Z, Su Y. Dimension reduction of large-scale second-order dynamical systems via a second-order arnoldi method. *SIAM J. Scientific Computing* 2005; **26**:1692–1709.

[30] Duan G. *Analysis and Design of Descriptor Linear Systems*. Springer, 2010.

[31] Bond B. Stability-preserving model reduction for linear and nonlinear systems arising in analog circuit applications. PhD Thesis, Massachusetts Institute of Technology, Department of Electrical Engineering and Computer Science 2010.

[32] Newmark N. A method of computation for structural dynamics. *Journal of Engineering Mechanics* 1959; **85**:67–94.

[33] Benner P, Feng L. Model Order Reduction for Coupled Problems. *Applied and Computational Mathematics: an international journal* 2015; **14**:3–22.

[34] Felippa C, Park K, Farhat C. Partitioned analysis of coupled mechanical systems. *Computer Methods in Applied Mechanics and Engineering* 2001; **190**:3247–3270.

[35] Farhat C, Rallu A, Wang K, Belytschko T. Robust and provably second-order explicit–explicit and implicit–explicit staggered time-integrators for highly non-linear compressible fluid–structure interaction problems. *International Journal for Numerical Methods in Engineering* 2010; **84**:73–107.

[36] Dettmer W, Perić D. A new staggered scheme for fluid–structure interaction. *International Journal for Numerical Methods in Engineering* 2013; **93**:1–22.

[37] de Oliveira L, da Silva M, Mosquera Sánchez J, Gonçalvez L. Loudness scattering due to vibro-acoustic model variability. *Journal of the Brazilian Society of Mechanical Sciences and Engineering* 2012; **34**:604–611.

[38] Hermann J, Junge M, Gaul L. Model Reduction and Substructuring Techniques for the Vibro-Acoustic Simulation of Automotive Piping and Exhaust Systems. *Proceedings of the IMAC-XXVIII, Jacksonville, Florida USA*, 2010; 1055–1064.

[39] Wyatt S. Issues in Interpolatory Model Reduction: Inexact Solves, Second-order Systems and DAEs. PhD Thesis, Faculty of the Virginia Polytechnic Institute and State University 2012.

DOI: 10.1002/nme

[40] Grimme E. Krylov projection methods for model reduction. PhD Thesis, ECE Department, University of Illinois 1997.

[41] Chung J, Hulbert G. A Time Integration Algorithm for Structural Dynamics With Improved Numerical Dissipation: The Generalized-alpha Method. *Journal of Applied Mechanics* 1993; **60**:371–375.

plate Young's modulus	69 GPa
plate Poisson's ratio	0.3
plate density	2700 kg/m^3
air density	1.225 kg/m^3
Rayleigh coefficient α	25
Rayleigh coefficient β	$2.5 \,.\, 10^{-7}$

Table I. Material properties of the aluminium plate and acoustic fluid.

roof Young's modulus	200 GPa
roof Poisson's ratio	0.3
roof density	8000 kg/m^3
air density	1.225 kg/m^3
seats normal impedance	$2 \,.\, 1.225 \,.\, 340$ Pa.s/m
Rayleigh coefficient α	10
Rayleigh coefficient β	$1 \,.\, 10^{-7}$

Table II. Material properties of the car interior and flexible roof.

DOI: 10.1002/nme